A bias-corrected CMIP5 dataset for Africa using CDF-t method. A contribution to agricultural impact studies.

Adjoua Moise Famien[1,2], Serge Janicot[2], Abe Delfin Ochou[1], Mathieu Vrac[3], Dimitri Defrance[2,5], Benjamin Sultan[2,5], and Thomas Noël[4]

[1]Université Félix Houphouët Boigny, LAPAMF-UFR SSMT, 22 BP 582, Abidjan 22, Ivory Coast
[2]UMR 7159 LOCEAN, Sorbonne Universités UPMC-CNRS-IRD-MNHN, Paris, France
[3]LSCE-IPSL, CNRS/CEA/UVSQ, Centre d'Études de Saclay, Orme des Merisiers, Gif-sur-Yvette, France
[4]Climate Data Factory, Paris, France
[5]ESPACE-DEV, Université Montpellier, IRD, Université Guyane, Université Réunion, Université Antilles, Université Avignon, Montpellier, France

Correspondence to: Serge Janicot (serge.janicot@locean-ipsl.upmc.fr)

Abstract. The objective of this paper is to present a new data set of bias-corrected CMIP5 global climate models (GCMs) daily data over Africa. This dataset was obtained using the Cumulative Distribution Function Transform (CDF-t) method, a method that has been applied on several regions and contexts but never on Africa. Here CDF-t has been applied over the period 1950-2099 combining Historical runs and climate change scenarios, on 6 variables, precipitation, mean near-surface air temperature, near-surface maximum air temperature, near-surface minimum air temperature, surface down-welling shortwave radiation, and wind speed, which are critical variables for agricultural purposes. WFDEI has been used as the reference dataset to correct the GCMs. Evaluation of the results over West Africa has been carried out on a list of priority users-based metrics that was discussed and selected with stakeholders. It includes simulated yield using a crop model simulating maize growth. These bias-corrected GCMs data have been compared with another available dataset of bias-corrected GCMs using WFD as the reference dataset. The impact of WFD, WFDEI and also EWEMBI reference datasets has been also examined in details. It is shown that CDF-t is very effective to remove the biases and to reduce the high inter-GCMs scattering. Differences with other bias-corrected GCMs data are mainly due to the differences between the references datasets. This is particular true for surface down-welling shortwave radiation, which has a significant impact in terms of simulated maize yields. Projections of future yields over West Africa are quite different, depending on bias-correction method used. However all these projections show a similar relative decreasing trend over the 21st century.

1 Introduction

Global (GCMs) and regional (RCMs) climate models are used to produce projections of future climates driven by various types of greenhouse gas emission scenarios. The last Coupled Model Intercomparison Project (CMIP ; Meehl et al., 2000), CMIP5, provides simulations for preindustrial period (CO_2 concentration at a level of 280 ppm), historical period (1860-2005; including real evolutions of CO_2 and other greenhouse gas concentrations, anthropogenic and volcanoes eruptions aerosols contents, solar activity), and future climate projections based on different CO_2 emission trajectory scenarios, Representative Concentration Pathways RCPx.x (Moss et al. 2010; x.x corresponding to the radiative forcing in $\mathrm{W\,m^{-2}}$ in 2100), RCP2.6, RCP4.5, RCP6.0 and RCP8.5 (Taylor et al., 2012).

Scientific communities working on evaluation and modelling of climate change impacts (in terms of crop yields, water resources, health, etc) are increasingly using these simulations outputs either to compute related impact metrics or to run impact models. However robust biases are still present in climate models due to ill-defined processes and associated parametrisations, leading to biased statistical distributions of simulated physical and dynamical variables (e.g., Vrac and Friederichs, 2015). Then statistical bias-corrections must be applied on variables used in impact models simulations (Vrac et al., 2016). For instance warmer than normal sea surface temperatures in the equatorial Atlantic leads to a too southern location of the ITCZ in boreal summer over West Africa. This bias has not been reduced between CMIP3 and CMIP5 GCM simulations (see Roehrig et al., 2013). This too southern ITCZ location over West Africa leads to too weak precipitation over the Sahel and too weak crop yields whose values cannot be used as relevant information for stakeholders and farmers.

GCMs and RCMs output data have to be adjusted to statistical distributions of observation based reference data. However, the use of different bias-correction methods in combination with different reference data sets contributes to the total uncertainty in climate projections and can contribute in some contexts more than the use of different GCMs or RCMs (Iizumi et al., 2017). So using multiple bias-correction technics and reference data sets can be recommended. For instance, a bias-correction of a subset of 5 GCMs of the CMIP5 database was realised at a global scale through the ISIMIP project (Hempel et al., 2013), the first Inter-Sectorial Impact Model Intercomparison Project[1]. These corrections were applied at a daily scale from 1 January 1950 to 31 December 2099, on Historical and all RCPs scenarios on 5 GCMs at a 0.5°x 0.5°grid, using WFD data as observation-based reference. More recently a ISIMIP2b bias-correction using an improved reference data set EWEMBI has been realized on 3 out of the 5 CMIP5 GCMs data, and the results have been compared to the bias-corrected ISIMIP/WFD data (Lange, 2017a). Significant differences have been highlighted that are closely related to differences between WDF and EWEMBI data.

The objectives of this paper are to present and evaluate bias-corrected GCMs data obtained by performing the Cumulative Distribution Function Transform (CDF-t) method over Africa, to quantify the sensitivity of the bias-corrected data to different reference datasets and to illustrate this in terms of simulated crop yields. It is a contribution to the AMMA-2050[2] project, centred on West Africa whose goals are to significantly improve scientific understanding of climate variability and change across Africa and the impact of climate change on specific development decisions, to introduce flexible methods for integrating improved climate information and tools in specific decision-making contexts and to improve medium-to long-term (5-40 year) decision-making, policies, planning and investment by African stakeholders and donors.

[1] https://www.isimip.org/
[2] http://www.amma2050.org/

Bias-correction has been applied on daily data of six variables critical for these types of impact: precipitation (pr), mean near-surface air temperature (tas), near-surface maximum air temperature (tasmax), near-surface minimum air temperature (tasmin), surface down-welling shortwave radiation (rsds), and wind speed (wind). The bias-correction has been performed using the Cumulative Distribution Function-transform (CDF-t ; Michelangeli et al., 2009), a method that has been widely used and validated for various variables and in various contexts (e.g., Kallache et al., 2011; Vrac et al., 2012; Lavaysse et al., 2012; Vautard et al., 2013; Vrac and Friederichs, 2015; Vrac et al., 2016), including tropical areas (Oettli et al., 2011; Vigaud et al., 2013) but not Africa. These corrections have been applied on 29 GCMs over 1950-2005 period and RCP2.6, RCP4.5 and RCP8.5 2006-2099 projections. The observation-based reference dataset used for bias-corrections is WFDEI, the WATCH Forcing Data (WFD; Weedon et al., 2011) methodology applied to ERA-Interim data, for the period from 1 January 1979 to 31 December 2013 on a 0.5°x 0.5°grid (Weedon et al., 2014).

Section 2 presents the reference data. A first intercomparison of WFD, WFDEI and EWEMBI is presented is terms of mean seasonal fields over West Africa. In Section 3 the CDF-t bias-correction method is shortly presented. Then tests are carried out over 1979-2013 to evaluate the sensitivity of the corrections to the calibration period. In section 4, the evaluation of the CDF-t bias-correction is detailed over West Africa, first on mean seasonal fields, then on daily-based metrics. CDF-t bias-corrected GCM data are also compared with ISIMIP/WFD bias-corrected data for the 5 GCMs used in ISIMIP. The significant impact induced by some improvements introduced in WFDEI data will be shown. CDF-t outputs are also compared to products from EWEMBI. To go further into this evaluation, a crop model has been used to test the impact on simulated crop yields (specifically a local maize cultivar) of bias-corrections data with one GCM and of the three reference data. A sensitivity analysis to individual forcing variables (temperature, precipitation and surface down-welling shortwave radiation) is also presented. Finally the bias-correction impact on crop simulations in the context of RCP8.5 climate change projections is shown. Conclusions are given in section 5.

2 Climate input data

The AMMA-2050 data set comprises bias-corrected daily data for the variables precipitation, mean near-surface air temperature, maximum air temperature and minimum air temperature, surface down-welling shortwave radiation, and wind speed. It covers the domain 20°W-55°E/40°S-40°N, including the whole Africa. In this paper, results are presented for West Africa (20°W-20°E/0-25°N) in boreal summer as it is the focus of AMMA-2050.

2.1 Simulations

We use daily data extracted from the CMIP5 archive, covering the period from 1 January 1950 to 31 December 2099. Based on availability of daily data, it comprises 29 GCMs for the 1950-2005 historical period and RCP8.5 2006-2099 projection, 27 GCMs for RCP4.5 projection and 20 GCMs for RCP2.6 projection (See Table 1 for more details). Only one run has been used for each GCM. For an easier comparison with observation, these “raw” data have been interpolated on the 0.5°x

Table 1. List of available CMIP5 models used for historical and RCP simulations. The 5 GCMs also used in ISIMIP are in italics. A number in each column is the number of ensemble member used in this work. Zero indicates that no run was used. The last line shows the total number of run used for each simulation.

Modelling Centre (or Group)	CMIP5 Models	Resolution (lat x lon x lev)	Simulations Historical	RCP2.6	RCP4.5	RCP8.5
Commonwealth Scientific and Industrial Research Organization (CSIRO) and Bureau of Meteorology (BOM), Australia	ACCESS1-0	1.25°x 1.875°x 38	1	0	1	1
	ACCESS1-3		1	0	1	1
Beijing Climate Center, China Meteorological Administration	bcc-csm1-1	1.875°x 1.875°x 16	1	1	1	1
	bcc-csm1-1-m		1	1	1	1
College of Global Change and Earth System Science, Beijing Normal University	BNU-ESM	2.81°x 2.81°x 26	1	1	1	1
Canadian Centre for Climate Modelling and Analysis	CanESM2	2.790°x 2.81°x 35	1	1	1	1
Centro Euro-Mediterraneo per I Cambiamenti Climatici	CMCC-CESM	3.443°x 3.75°x 39	1	0	0	1
	CMCC-CM	0.748°x 0.75°x 31	1	0	1	1
	CMCC-CMS	3.711°x 3.75°x 95	1	0	1	1
Centre National de Recherches Météorologiques/Centre Européen de Recherche et Formation Avancée en Calcul Scientifique	CNRM-CM5	1.4°x 1.4°x 31	1	1	1	1
Commonwealth Scientific and Industrial Research Organization in collaboration with Queens land Climate Change Centre of Excellence	CSIRO-Mk3-6-0	1.875°x 1.875°x 18	1	1	1	1
NOAA Geophysical Fluid Dynamics Laboratory	GFDL-CM3	2°x 2.5°x 48	1	1	1	1
	GFDL-ESM2G	2°x 2.5°x 24	1	1	1	1
	GFDL-ESM2M	2°x 2.5°x 24	1	1	1	1
Met Office Hadley Centre (additional HadGEM2-ES realizations contributed by Instituto Nacional de Pesquisas Espaciais)	HadGEM2-AO	1.25°x 1.875°x 38	1	1	1	1
	HadGEM2-CC	1.25°x 1.875°x 38	1	0	1	1
	HadGEM2-ES	1.25°x 1.875°x 38	1	1	1	1
Institute for Numerical Mathematics	Inmcm4	1.5°x 2°x 21	1	0	1	1
Institut Pierre-Simon Laplace	IPSL-CM5A-LR	1.9°x 3.75°x 39	1	1	1	1
	IPSL-CM5A-MR	1.25°x 2.5°x 39	1	1	1	1
	IPSL-CM5B-LR	1.9°x 3.75°x 39	1	0	1	1
Atmosphere and Ocean Research Institute (The University of Tokyo), National Institute for Environmental Studies, and Japan Agency for Marine-Earth Science and Technology	MIROC5	1.4°x 1.4°x 40	1	1	1	1
Japan Agency for Marine-Earth Science and Technology, Atmosphere and Ocean Research Institute (The University of Tokyo), and National Institute for Environmental Studies	MIROC-ESM	2.8125°x 2.8125°x 80	1	1	1	1
	MIROC-ESM-CHEM		1	1	1	1
Max-Planck-Institut für Meteorologie (Max Planck Institute for Meteorology)	MPI-ESM-LR	1.8653°x 1.875°x 47	1	1	1	1
	MPI-ESM-MR	1.8653°x 1.875°x 95	1	1	1	1
Meteorological Research Institute	MRI-CGCM3	1.12148°x 1.125°x 48	1	1	1	1
	MRI-ESM1		1	0	0	1
Norwegian Climate Centre	NorESM1-M	1.9°x 2.5°x 26	1	1	1	1
Total	**29**		**29**	**20**	**27**	**29**

0.5°grid of WFDEI by a bilinear approach for temperatures and wind, and by a “nearest neighbour” approach for precipitation. Then, bias-corrected data are available on the 0.5°x 0.5°grid.

2.2 Reference observation data sets

The observation-based reference dataset is critical for the correction of GCM biases, especially when corrections are applied on daily data. The reference dataset must also have a global coverage on a regular grid, what may induce large uncertainties in void in-situ data areas as in Africa. So we used the opportunity of the availability of WFD, WFDEI and EWEMBI reference datasets to compare each other, and to compare bias-corrected (with WFD) ISIMIP data with bias-corrected (with WFDEI) AMMA-2050 data.

The WFD dataset (Weedon et al., 2011) is a combination of ERA-40 daily reanalysis of the European Centre for Medium-Range Weather Forecasts (ECMWF) at a grid resolution of 2.5°and the Climate Research Unit (CRU) TS2.1 dataset that provides observed time series of monthly variations in the climate on a resolution grid of 0.5°. A correction for monthly mean rainfall is included using the Global Precipitation Climatology Centre (GPCC) version 4 dataset (Hagemann et al., 2011). The WFD data are available over the period 1958-2001 on a 0.5°grid over land area points. WFD dataset has been used over 1979-2001.

WFDEI, an improved version of WFD, has been produced based on ERA-Interim reanalysis, over the period from 1 January 1979 to 31 December 2013 on a 0.5°x 0.5°grid (Weedon et al., 2014). Improvements come from the 4D-var data assimilation system with 6h windows in ERA-Interim instead of 3D-var in ERA-40. Compared to ERA-40, ERA-Interim uses a more extensive suite of satellite, atmospheric soundings and surface observations and provides substantial improvement in surface meteorological variables (Dee et al., 2011), in particular with a new aerosol loading distributions and corrections for downward shortwave fluxes (leading in particular to larger average WFDEI values over Sahara and northern Africa) leading to less bias compared to globally distributed observations. ERA-Interim has also a reduced Gaussian grid spectral model resolution of T255 instead of T159 for ERA-40, leading to data much “closer” to the regular 0.5°x 0.5°spatial resolution and to the elevation distribution used for WFDEI. A correction for monthly mean rainfall is included using the GPCCv5/v6 dataset. WFDEI dataset has been used over 1979-2013.

More recently, the EWEMBI data set has been produced within ISIMIP (Lange, 2016, 2017b). Over land, EWEMBI is identical to the WFDEI dataset for precipitation, daily mean, minimum and maximum near-surface air temperature and 10 m wind speed, but different for surface downwelling shortwave radiation. Data sources of EWEMBI are ERA-Interim data, WFDEI, eartH2Observe forcing data (E2OBS; Dutra, 2015) and NASA/GEWEX Surface Radiation Budget data (SRB; Stackhouse Jr et al., 2011) primary-algorithm estimates of daily mean rsds from SRB release 3.0 (Frieler et al., 2017; Lange, 2017b). Significant differences have been highlighted between WFD-based and EWEMBI-based bias-corrected data that are closely related to similar improvements from WDF to EWEMBI data. EWEMBI dataset has been used over 1979-2013.

Table 2. Spatial correlation, standard deviation (STD) and root mean square error (RMSE) computed for differents observations dataset over Sahel box (18°W-10°E ; 10°N-20°N) and Guinea box (18°W-10°E ; 3°N-10°N) in JAS. All scores are computed relative to WFDEI for seasonal mean precipitation (Mean pr), seasonal near-surface air temperature (Mean tas), seasonal surface downwelling shortwave radiation (Mean rsds), the 95^{th} percentile of daily values for precipitation (R95p) and near-surface air temperature (T95p), the number of wet days (R1mm), the number of heavy days (R10mm), the number of dry days, the 95^{th} percentile of consecutives dry days and the number of day with tas greater than 30°C.

	SAHEL								
	Correlation			**STD**			**RMSE**		
Metrics	**WFDEI**	**WFD**	**EWEMBI**	**WFDEI**	**WFD**	**EWEMBI**	**WFDEI**	**WFD**	**EWEMBI**
Mean tas	-	0.997	1.000	2.797	2.581	2.797	-	0.414	0.000
Mean pr	-	0.999	1.000	3.176	3.237	3.176	-	0.203	0.000
Mean rsds	-	0.980	0.938	43.125	47.945	30.944	-	39.115	18.687
T95p	-	0.994	1.000	3.290	2.830	3.290	-	0.577	0.000
R95p	-	0.970	1.000	6.740	12.979	6.740	-	8.424	0.000
R10mm	-	0.965	1.000	3.751	3.202	3.751	-	3.214	0.000
Number of day with tas > 30°C	-	0.996	1.000	35.114	35.988	35.114	-	4.487	0.000
R1mm	-	0.961	1.000	27.421	15.859	27.421	-	21.527	0.000
Number of dry days	-	0.961	1.000	9.140	5.286	9.140	-	7.176	0.000
95^{th} percentile of CDD	-	0.977	1.000	9.800	5.618	9.800	-	6.609	0.000
	GUINEA								
	Correlation			**STD**			**RMSE**		
Metrics	**WFDEI**	**WFD**	**EWEMBI**	**WFDEI**	**WFD**	**EWEMBI**	**WFDEI**	**WFD**	**EWEMBI**
Mean tas	-	0.887	1.000	0.733	0.624	0.736	-	0.741	0.000
Mean pr	-	0.995	1.000	3.647	3.644	3.680	-	0.352	0.000
Mean rsds	-	0.824	0.390	15.387	14.419	13.946	-	54.940	28.532
T95p	-	0.844	1.000	0.789	0.655	0.795	-	1.005	0.000
R95p	-	0.948	1.000	7.866	11.735	7.957	-	13.676	0.000
R10mm	-	0.969	1.000	17.860	10.681	17.860	-	7.972	0.000
Number of day with tas > 30°C	-	0.571	1.000	0.005	0.075	0.005	-	0.075	0.000
R1mm	-	0.717	1.000	7.440	10.897	7.440	-	29.305	0.000
Number of dry days	-	0.717	1.000	2.480	3.632	2.480	-	9.768	0.000
95^{th} percentile of CDD	-	0.886	1.000	7.910	4.750	7.910	-	9.374	0.000

2.3 Intercomparison of WFD, WFDEI and EWEMBI on mean seasonal fields over West Africa

In the following, to reduce the number of figures, the results are presented only for the summer season, July-September (JAS), which is the main rainy season over the Sahel. Similar computations have been performed over the other seasons, especially over spring, which is the main rainy season over the Guinean Coast, and some of the results will be commented.

Fig.1 presents the July-September mean seasonal fields of WFD, WFDEI and EWEMBI for tas, pr and rsds. Regarding tas, the mean fields of the three reference data sets are very close, showing the set-up in northern spring and summer of the high temperature area associated to the Saharan and Saudi Arabia heat lows. Regarding pr, the seasonal fields are also very close,

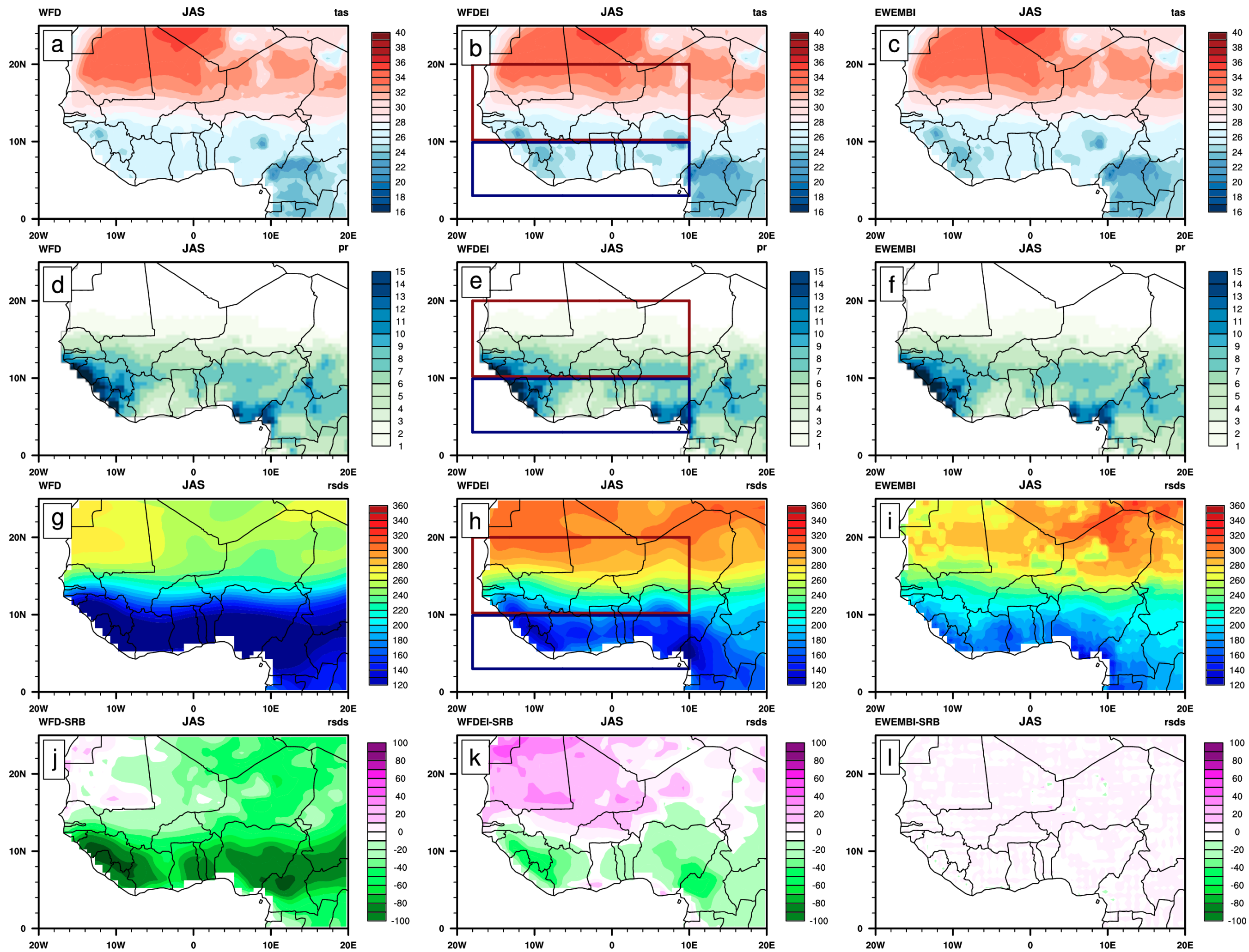

Figure 1. Summer climatology from different observations datasets (WFD, WFDEI and EWEMBI) : (a-c) for near-surface temperature (°C) over 1979-2001, (d-f) for precipitation rate ($\mathrm{mm\,day^{-1}}$) over 1979-2001 period, (g-i) for solar radiation ($\mathrm{W\,m^{-2}}$) over 1984-2001 period and difference between WFD (j) over 1984-2007, WFDEI (k) over 1984-2007, EWEMBI (l) over 1984-2001 and SRB solar radiation. The red box (18°W-10°E ; 10°N-20°N) and blue box (18°W-10°E ; 3°N-10°N) represents respectively Sahel and GUINEA regions used in this study.

showing the seasonal migration of the Inter-Tropical Convergence Zone (ITCZ) between spring and summer. Local maxima associated to highlands like Fouta Jalon or Cameroon mountains are also clearly highlighted. Regarding rsds, more differences are evident between the 3 reference data sets. The mean seasonal fields show similar patterns with low values within the ITCZ area due to the high cloud coverage and high values over the Sahara due to low moisture and cloud coverage, but the range of values are quite different. Over ITCZ WFD rsds values are the weakest and EWEMBI values the highest. Over the Sahara

WFD values are also the weakest but WFDEI values are a bit higher than for EWEMBI. In the remaining panels, differences are produced in respect to SRB data. Compared to SRB, EWEMBI data are very similar that is logical since SRB data was used to correct ERA-Interim. WFDEI has moderate negative biases in the ITCZ area and weak positive biases over the Sahara, while WFD has high negative biases over the whole area.

3 The CDF-transform bias-correction

3.1 The CDF-t method

In this work, we use the CDF-t method developed by Michelangeli et al. (2009) to adjust climate models. It consists in matching the CDF of a climate variable simulated by a model (here the GCM) to be corrected at the CDF of this observed variable (here WFDEI) through a mathematical function. CDF-t is a variant of the non-parametric Quantile-quantile (QQ) method (Déqué, 2007). But contrary to the QQ method that projects the GCM CDF of simulated future data onto the CDF of historical data, CDF-t considers the CDF change between GCM historical and future simulations. Let $\mathrm{F_{Gh}}$ and $\mathrm{F_{Sh}}$ define the CDFs of a variable from the GCM (subscript G) and from a given reference location (subscript S) over a historical calibration period (subscript h). The transformation T allows to go from $\mathrm{F_{Gh}}$ to $\mathrm{F_{Sh}}$:

$$T(\mathrm{F_{Gh}}(x)) = \mathrm{F_{Sh}}(x). \tag{1}$$

Replacing x by $\mathrm{F_{Gh}^{-1}}$(u), where u is any probability in [0, 1] :

$$T(u) = \mathrm{F_{Sh}}(\mathrm{F_{Gh}^{-1}}(u)), \tag{2}$$

which provides a definition of T. Assuming T is stationary in time, the transformation can be applied to $\mathrm{F_{Gf}}$, the CDF of the variable over a future or validation period f, to generate $\mathrm{F_{Sf}}$, the CDF at the reference location for the same period f :

$$T(\mathrm{F_{Gf}}(x) = \mathrm{F_{Sf}}(x), \tag{3}$$

That is :

$$\mathrm{F_{Sf}}(x) = \mathrm{F_{Sh}}(\mathrm{F_{Gh}^{-1}}(\mathrm{F_{Gf}}(x))). \tag{4}$$

Once $\mathrm{F_{Sf}}$ has been determined from (4), a QQ approach is carried out between $\mathrm{F_{Gf}}$ and $\mathrm{F_{Sf}}$ to generate local time series. While in (Déqué, 2007), QQ is applied directly between $\mathrm{F_{Gh}}$ and $\mathrm{F_{Sh}}$, the CDF-t method generates quantile values through a QQ performed between $\mathrm{F_{Gf}}$ (and not $\mathrm{F_{Gh}}$) and $\mathrm{F_{Sf}}$ (and not $\mathrm{F_{Sh}}$). Values are then generated according to $\mathrm{F_{Sf}}$ in chronological agreement with "future" climate simulations. More details on the CDF-t method can be found in (Vrac et al., 2012, 2016).

3.2 Application

This CDF-t approach has been applied to 5 out of the 6 variables (tas, tasmax, tasmin, rsds and wind) over the period 1950-2099 (historical and RCP2.6, RCP4.5, RCP8.5 runs). For precipitation (pr), an updated CDF-t approach has been used, referred to as “Singularity Stochastic Removal” (SSR), addressing also rainfall occurrence and intensity issues (see Vrac et al., 2016, for more details).

CDF-t has been applied month by month to take in account the strong seasonality over Africa. It has been applied using a moving window to smooth discontinuities (Vrac et al., 2016): a moving 17-year window is used as the “target” CDF, and the GCM data of the central 9 years are corrected. This process is repeated by moving forward the window by 9 years, covering then the whole period 1950-2099. Moreover CDF-t preserves any long-term trend in the GCM data but neither trends in moments nor in quantiles (Vrac et al., 2012). GCM data have been interpolated to WFDEI grid before being bias-corrected, using a bilinear method for tas, tasmax, tasmin, rsds and wind, and a nearest neighbour method for pr.

Examples of CDF-t bias-correction applied on mean West Africa daily precipitation data for the five GCMs used in ISIMIP are shown (Fig.S1). It is represented in terms of cumulative distribution function. The distributions of raw GCM data are clearly different from the WFDEI data. Some of them show more low precipitation values in GCMs than in WDFEI while others have more low precipitation values. The CDF-t bias-correction appears very effective as WFDEI and bias-corrected GCM data distribution are closely superimposed.

3.3 Sensitivity of the correction to the calibration period over West Africa

Before applying the CDF-t correction through the moving window process over 1950-2099, the bias-correction method has to be calibrated individually for every GCM over a reference period. In order to have a calibration data set as representative as possible of the variability of the various variables, especially precipitation, the time period 1979-2013 has finally been used for calibration of the bias-correction method. However the sensitivity to the calibration period has been explored over West Africa by testing it on two sub-periods, 1979-1996 and 1996-2013, to prevent any over-estimation of the bias-correction performance. This has been performed on the five GCMs used in ISIMIP, and it is more specifically shown on IPSL-CM5A-LR model in summer for tas, pr and rsds (Supplementary Information).

Three calibration periods have been tested: 1979-1996, 1996-2013 and 1979-2013 (see Fig.S2). First, it is clear that the bias-correction is powerful to remove the cold bias of the raw data. Second, the positive trend present in the raw data over the period 1979-2013, as in WFDEI but with a weaker range, is preserved after the bias-correction. This is probably due to the dry bias of precipitation over the Sahel in raw data that induces a higher sensitivity to the impact of anthropogenic global warming over the period than in observations. Third, the effect of the calibration period is clear. By using the calibration period 1979-1996, the remaining bias of corrected data is near zero and is weakly positive over 1997-2013, while by using the calibration period 1996-2013, the remaining bias of corrected data is near zero and is weakly negative over 1979-1995. Using the calibration period 1979-2013, the remaining bias is overall very weak and in average near zero. Similar tests have been carried out for the variables pr and rsds, and for the other seasons, with similar conclusions. So, while it can be thought that using the whole observational period to calibrate the bias-correction process may lead to over-estimation of the fit between observations and bias-corrected data, it provides in fact a more robust correction. So we choose the longest period 1979-2013 to perform calibration process.

4 Results

4.1 User-based metrics and diagnostics

A list of priority metrics has been established between scientists and stakeholders involved in AMMA-2050. We are presenting results based on some of these metrics related to the three variables, precipitation (pr), near-surface air temperature (tas) and surface down-welling shortwave radiation (rsds). These metrics are:

- the seasonal mean for pr, tas and rsds,
- the mean time-latitude annual cycle over (15°W-15°E) for pr, tas and rsds,
- the 95$^{\text{th}}$ percentile of daily values for tas,
- the number of days with tas > 30°C,
- the 95$^{\text{th}}$ percentile of daily values for pr,
- the number of wet days (pr > $1\ \mathrm{mm\,day^{-1}}$),
- the number of days with pr > $10\ \mathrm{mm\,day^{-1}}$,
- the number of dry days (pr < $1\ \mathrm{mm\,day^{-1}}$),
- the 95$^{\text{th}}$ percentile of the duration of consecutive dry days sequences.

4.2 Mean seasonal fields over West Africa

In the following, the Taylor diagram (Taylor, 2001) will be used to quantify the distance between the raw, bias-corrected GCMs data and WFDEI data. This diagram provides three statistics, the spatial correlation coefficient between the tested field and the reference field, the normalized standard deviation of the tested field in respect to the standard deviation of the reference field, and the centred root mean square difference (RMSE) between the tested field and the reference field. The Taylor diagram has been also used to evaluate the distance between the reference datasets WFD and EWEMBI relative to WFDEI. Table 2 sums up the three Taylor's statistics of these reference datasets for all the metrics.

Regarding the seasonal mean metrics, WFDEI and EWEMBI statistics are similar except for rsds where they are quite different over the Guinean coast. WFD is also very close to WFDEI but all statistics are a bit different, with again more differences for the Guinea coast.

Fig.2 presents the mean JAS temperature fields over West Africa for WFDEI data and for raw data from the five GCMs used in ISIMIP. Fig.S3 shows similar fields but for CDF-t bias-corrected data. Fig.3 shows the Taylor diagrams computed on JAS over the Sahel and Guinea areas, for the 29 raw and bias-corrected GCMs data compared to WFDEI data (first column), and the five GCMs used in ISIMIP in terms of raw data of CDF-t bias-corrected data and of ISIMIP bias-corrected data (second column). WFD and EWEMBI data are also plotted in these diagrams. In the Taylor diagrams the mean of the fields

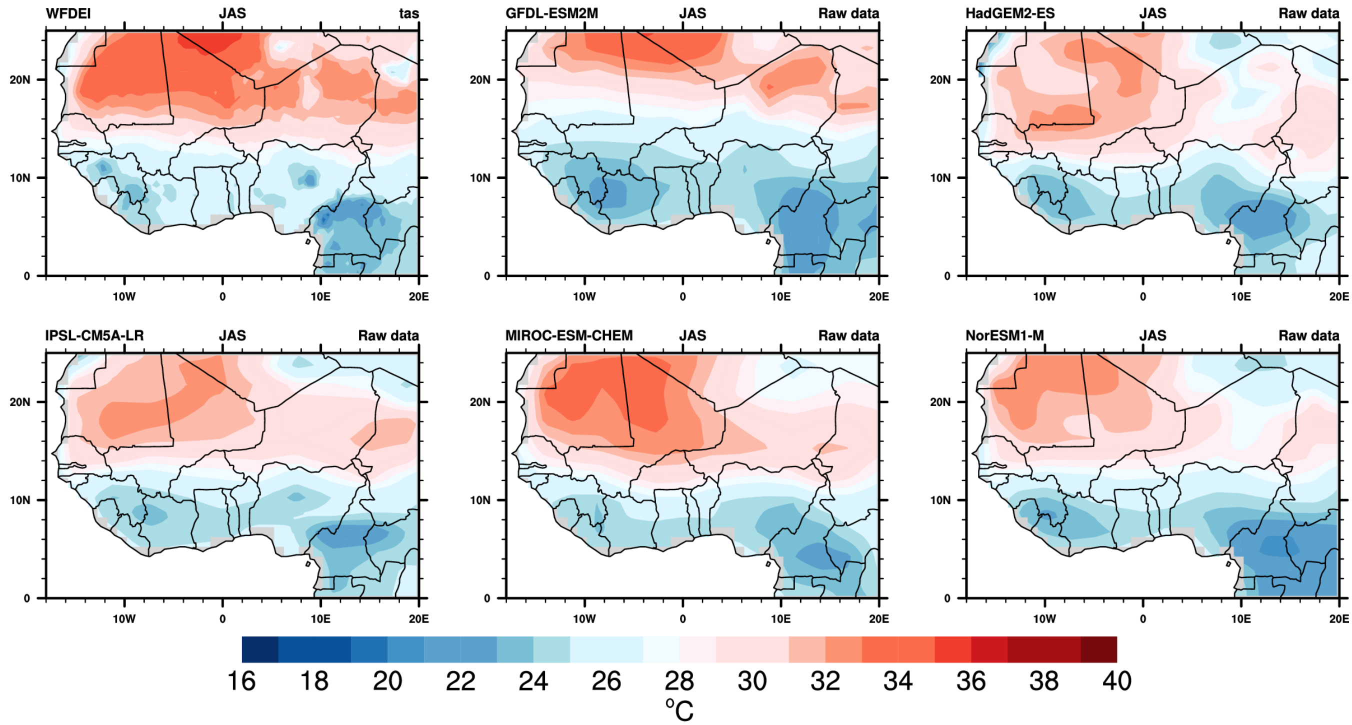

Figure 2. Mean near-surface air temperature (°C) in JAS 1979-2001 from WFDEI and from 5 CMIP5 GCMs raw data (the GCMs also used in ISIMIP).

are subtracted out before computing their second-order statistics, so these diagrams do not provide information about overall biases but characterizes biases associated to centred pattern errors. Hence maps of Fig.2 and Taylor diagrams of Fig.3 provide complementary bias information.

Fig.2 shows that the raw GCMs capture rather well the spatial structure of temperature over Africa, characterized by high values over the Sahara in summer as well as in spring (not shown), and low values in northern fall and winter (not shown). However moderate cold biases exist over most of the area. Inter-model dispersion is also present. For instance temperatures in MIROC-ESM-CHEM are about 2°C higher than temperatures in HadGEM2-ES or IPSL-CM5A-LR. The bias-correction process improves quite well the simulations (see Fig.S3) and provides corrected mean seasonal fields very similar to WFDEI, even at small spatial scales as for lower temperatures over Fouta-Jalon and Cameroon mountains. The Taylor diagrams (Fig.3) quantify this improvement very clearly for the 29 GCMs. The raw GCMs (Fig.3 left column) are quite scattered with spatial correlations with WFDEI distributed between +0.1 to more than +0.9. For the Sahel area, correlations are quite high in JAS (centred around +0.9 between 0.5 and 0.98), while for the Guinean area correlations are globally centred around +0.4 (from 0.1 to 0.8). GCMs are also scattered in terms of normalized variances, from 0.6 to more than 2. The performance of the CDF-t bias-correction is clearly high since all the GCMs are very close to the WFDEI reference point. Taylor diagrams enable to compare the 5 GCMs used in ISIMIP in reference to WFDEI (Fig.3 right column), for raw data, bias-corrected data by CDF-t

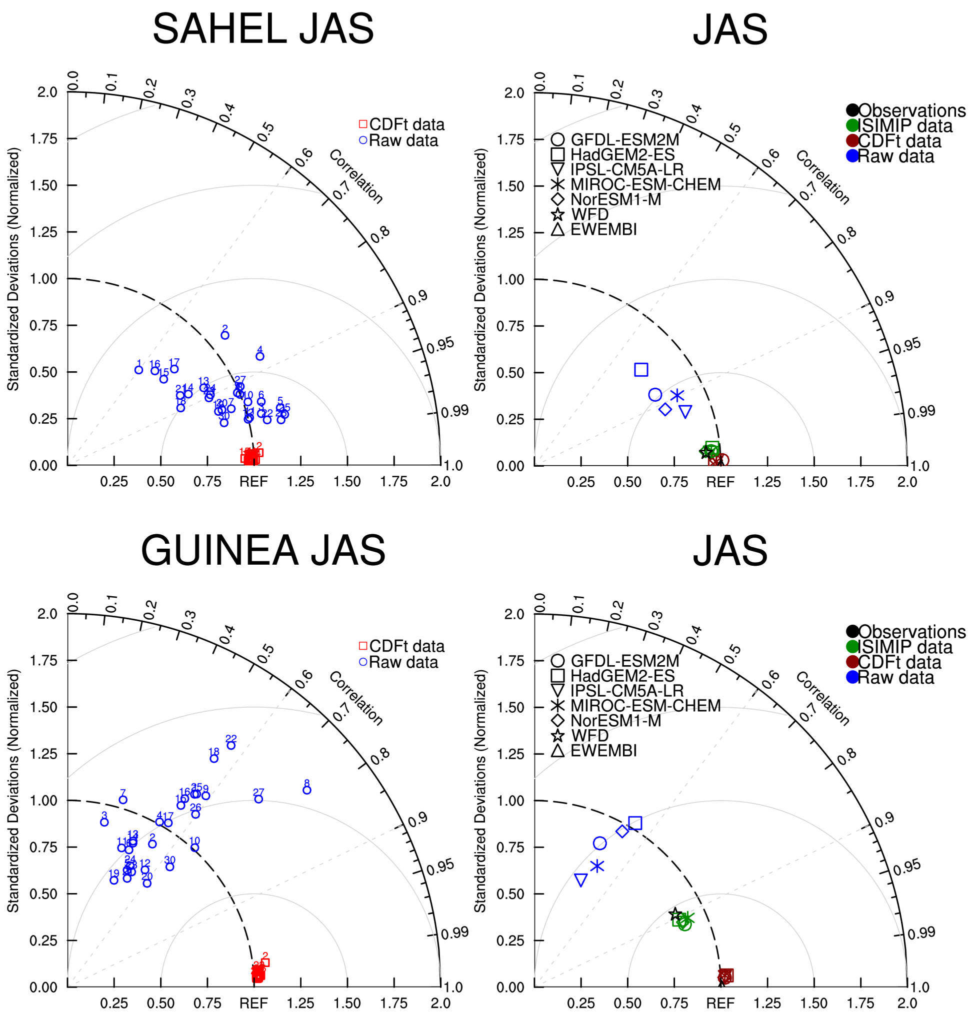

Figure 3. Taylor diagrams relative to the mean of near-surface air temperature over 1979-2001 from 29 individual models (first column) and 5 out of them (second column) used also in ISIMIP. Two areas are considered: Sahel and Guinea boxes (see these boxes on Fig.1, Fig.18 or Fig.19). Data are compared to WFDEI data. Taylor diagrams provide three statistics: the correlation coefficient between any tested field and the reference field (related to the azimuthal angle), the normalized standard deviation of the tested field in respect to the standard deviation of the reference field (proportional to the radial distance from the origin), and the centred root mean square difference between the tested field and the reference field (proportional to the distance from the REF point on the x-axis; grey circles from 1 (with the lowest radius) to 4 (the highest radius)). “Observations” label represents WFD and EWEMBI data (in black). Raw GCMs data are in blue, CDF-t bias-corrected GCMs data in red and ISIMIP bias-corrected GCMs data in green.

and by ISIMIP method. WFD and EWEMBI data are also plotted. CDF-t bias-corrected GCMs are very close to WFDEI. ISIMIP bias-corrected GCMs are centred around WFD and also near to WFDEI (correlation higher than +0.9 and normalized

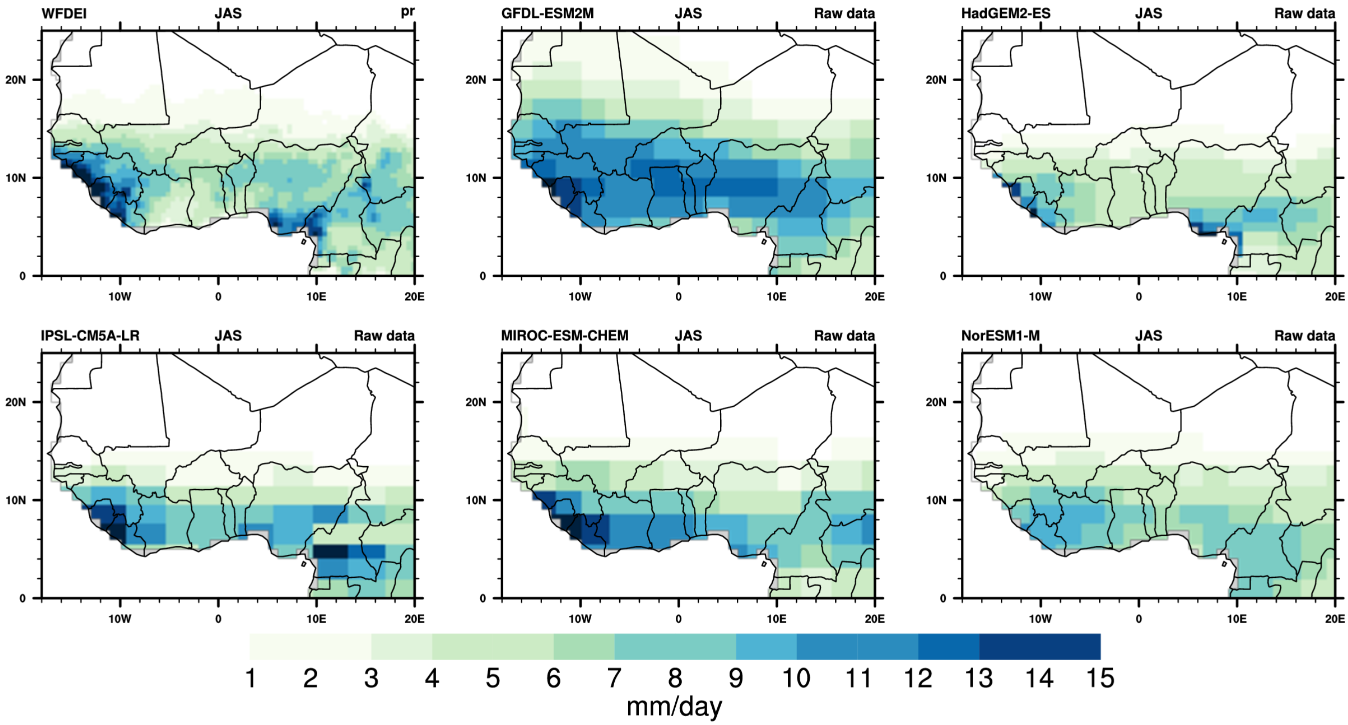

Figure 4. Same as Figure 2 but for precipitation rate in $\mathrm{mm\,day^{-1}}$

standard deviation close to 1) ; however WFD is a bit more distant to WFDEI for the Guinean area (see also Table 2). EWEMBI data is even more close to WFDEI.

Fig.4, Fig.5 and Fig.S4 show similar results but for pr. The seasonal fields of WFDEI show the mean location of the ITCZ in JAS (Fig.4). Local maxima associated to highlands like Fouta Jalon or Cameroon mountains are also clearly highlighted. Raw GCMs reproduce this pattern but a lot of discrepancies can be noticed for all GCMs, both in terms of precipitation amplitude, spatial pattern and latitude extension. HadGEM2-ES has the weakest values while the four others produce precipitation amounts generally higher than WFDEI. The CDF-t bias-correction improves very efficiently the GCM mean seasonal precipitation fields since examination must be very detailed to discern differences with WFDEI fields and between the GCMs (see Fig.S4). This improvement is clearly quantified with the Taylor diagrams over Sahel and Guinea areas in Fig.5. For raw GCMs the standardized standard deviation is very scattered from 0.25 to more than 2. Spatial correlations are higher in Sahel (from +0.7 to +0.95) than in Guinea area (from +0.2 to +0.8). The CDF-t bias-correction is quite effective in removing these biases and bringing the raw data closer to WFDEI, with some small remaining discrepancies, higher than for tas. The ISIMIP bias-correction is also effective due to the proximity between WFD and WFDEI (see also Table 2).

Fig.6, Fig.7 and Fig.S5 show similar results, but for rsds. The mean seasonal field of WFDEI is a pattern with low values within the ITCZ area due to the high cloud coverage and high values on Sahara due to low moisture and cloud coverage. We have noticed previously (Fig.1) that high differences exist between WFDEI, WFD and EWEMBI. WFD rsds values are the

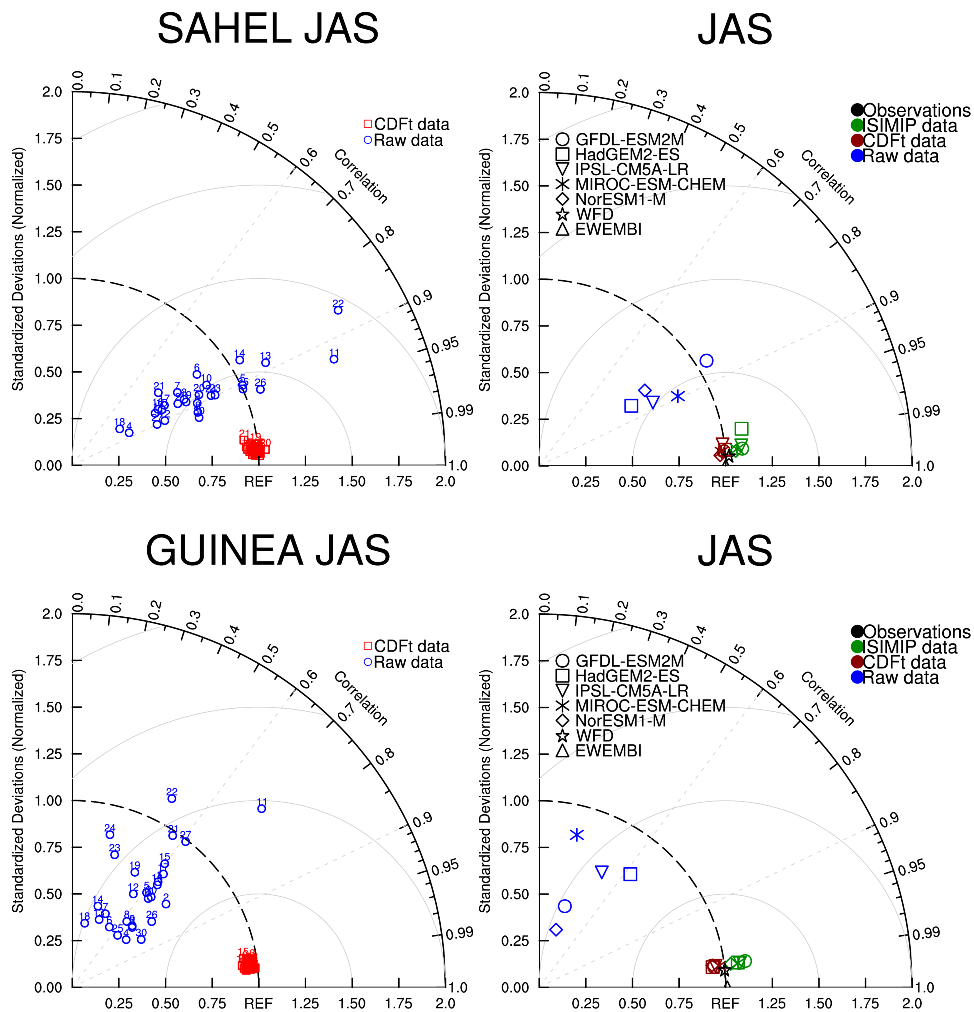

Figure 5. Same as Figure 3 but for precipitation rate

weakest and EWEMBI values the highest in the ITCZ area. WFD values are also the weakest and WFDEI values are a bit higher than for EWEMBI over the Sahara (see also Table 2). The five raw GCMs have, in agreement with their precipitation mean seasonal fields, a reasonable latitudinal evolution of low rsds values associated to the ITCZ, but the range of rsds differences with WFDEI data as well as the inter-GCMs dispersion are very high. There is an overall positive bias over West Africa, except for GFDL-ESM2M. The CDF-t bias-correction is once more very effective to remove biases respect to WFDEI data (see Fig.S5). The Taylor diagrams (Fig.7) provide some more quantification over the Sahel and Guinea areas. In terms of spatial correlation and normalized standard deviation in respect to WFDEI, raw GCMs have rather good performances over the Sahel (correlations higher than +0.8). Again, results are less good over the Guinea area (correlations less than +0.8) with a high dispersion of the GCMs. The ISIMIP bias-correction reduces highly the inter-GCMs dispersion around WFD, but WFD rsds data is a bit far from WFDEI rsds data. EWEMBI rsds data are also far from WFDEI. This is illustrated on the Taylor

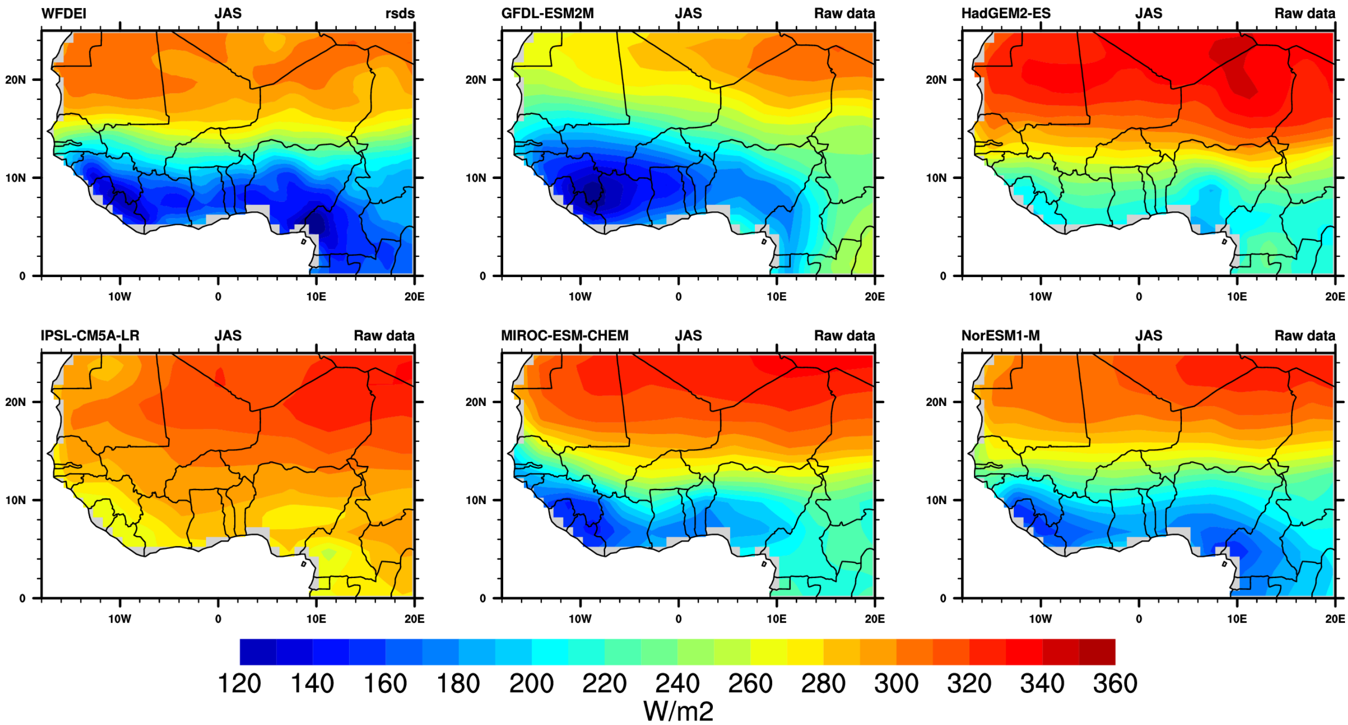

Figure 6. Same as Figure 2 but for solar radiation in $\mathrm{W\,m^{-2}}$

diagnostics using EWEMBI as "REF". Both bias-corrected data from CDF-t and ISIMIP method stay far from EWEMBI and do not improve the performance of raw GCMs.

Fig.8 to Fig.10 display other features of the mean fields in terms of Hovmoëller diagrams computed over West Africa (15°W-15°E) for the whole year. They show the mean fields of EWEMBI, WFDEI and WFD (first row), and of the five GCMs used in ISIMIP (row 2 to 6) for raw data (first column), CDF-t bias-corrected data (second column) and ISIMIP bias-correction method (third row). For tas (Fig.8), the WFDEI, WFD and EWEMBI fields are very similar and highlight the set-up of the high temperatures area associated with the Saharan heat low in spring and summer (Lavaysse et al., 2009). Raw GCMs show a similar timing but their temperature values are lower by 2°C to 4°C depending on the model, and some increase of the northward progression around June that is not present in observations. Bias-correction methods are very effective to reduce these discrepancies but few differences still remain with WFDEI as for instance a bit weaker temperature maximum around July in CDF-t corrected data. ISIMIP bias-corrected data are also very closer to WFD.

Fig.9 shows similar diagrams but for pr. The Hovmoeller approach is a good way to depict the main characteristics of the ITCZ evolution over West Africa with a first rainy season during spring over the Guinea area followed by an "abrupt jump" to the north in June-July (Sultan and Janicot, 2003) and by a more progressive southward retreat at the end of the summer monsoon season, leading in fall to a second weaker rainy season over the Guinean area. WFDEI and EWEMBI are quite similar. WFD fields are a bit noisier. Raw GCMs have high discrepancies and produce mean fields quite different from one

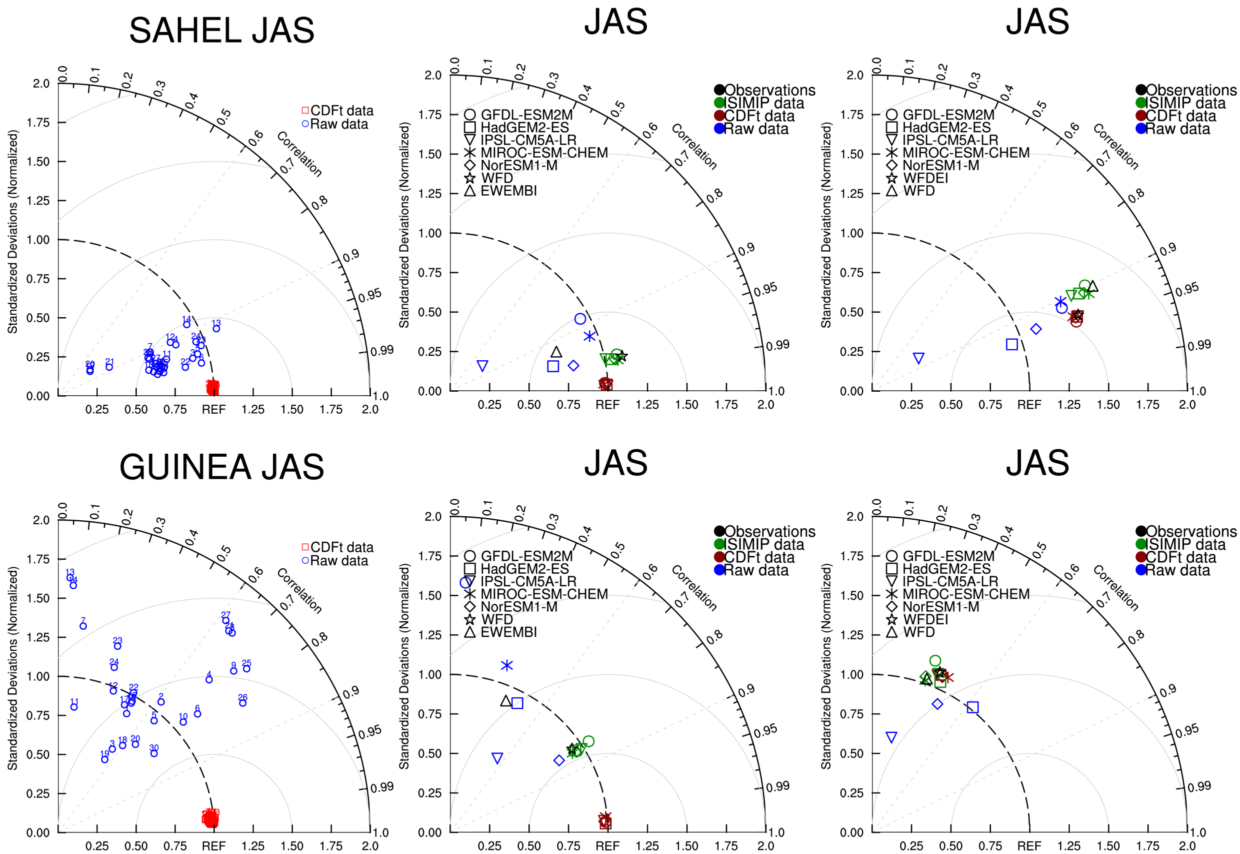

Figure 7. Same as Figure 3 but for solar radiation. In the right column, EWEMBI is used as "REF".

model to another one. In particular, precipitation data can be either very low (HadGEM2-ES) or very high (GFDL-ESM2M), and no GCM captures well the abrupt northward shift of the ITCZ. The bias-correction methods (CDF-t using WFDEI, ISIMIP using WFD) are very effective in capturing back the main features of the ITCZ evolution. However differences still remain between the GCMs, and ISIMIP corrected GCMs have globally rainfall maxima higher than CDF-t corrected GCMs.

Fig.10 shows similar diagrams but for rsds. The seasonal evolution is in agreement with tas and pr fields and depicts high solar radiation values over the Sahara, and weak values following the ITCZ latitudinal excursion but with a small southward lag (consistent with a higher cover of mid-level clouds, (see Roehrig et al., 2013)). WFD shows an overall negative bias with respect to WFDEI and EWEMBI, and WFDEI has a higher meridional gradient than EWEMBI with lower minimum values over the Guinea area and higher maximum values of the Sahara. The corrected GCM data are very close to their respective observation reference (WFD for ISIMIP, WFDEI for CDF-t), and hence different between their two respective corrected versions due to the differences between WFD and WFDEI.

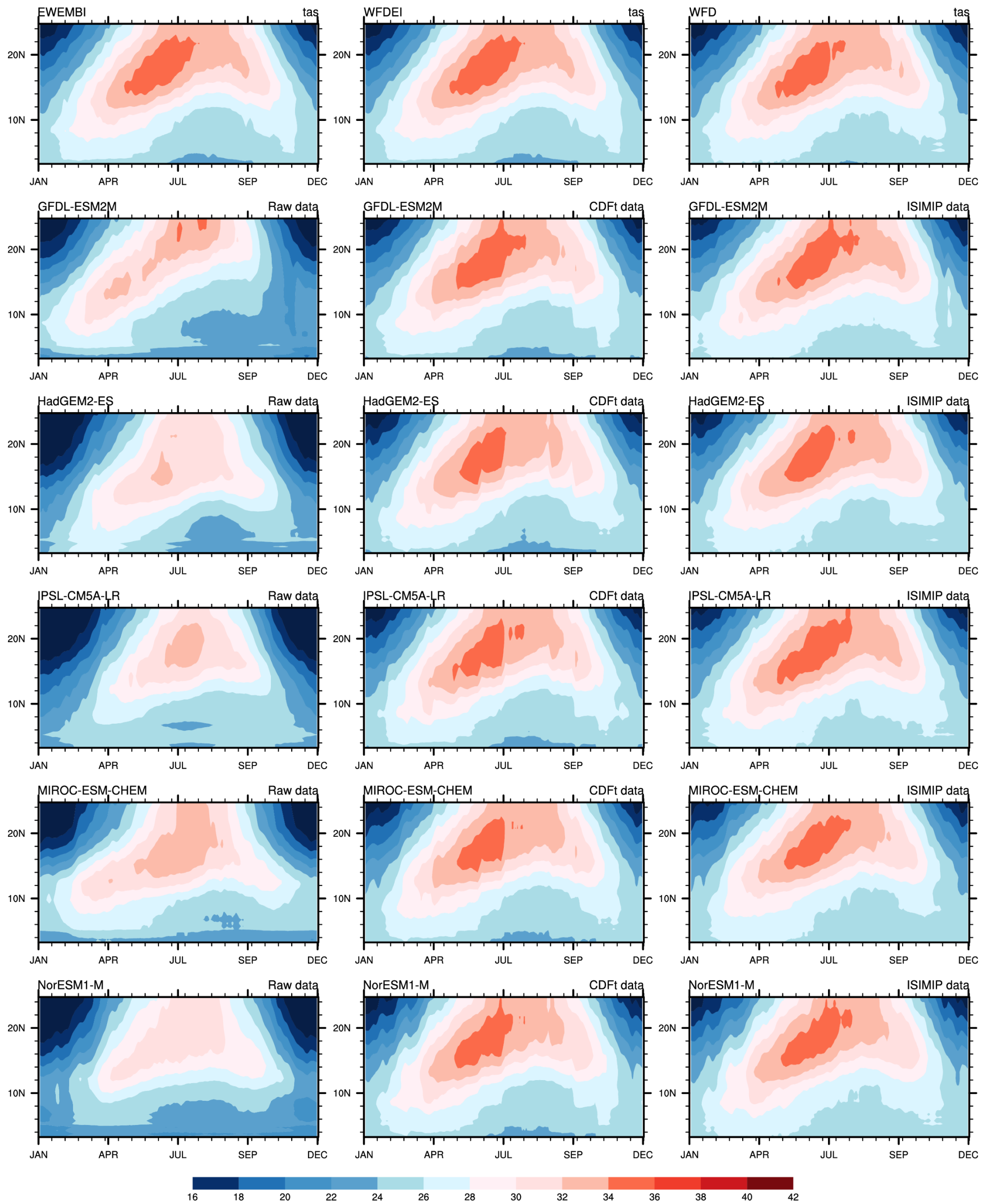

Figure 8. Hovmoëller diagrams of daily temperature (°C) averaged between 15°W and 15°E and for the period 1979-2001 for EWEMBI, WFDEI and WFD observations, each of the 5 GCMs for Raw data (1st column), CDF-t data (second column) and ISIMIP data (3rd column).

4.3 Daily-based metrics over West Africa

In the following, similar diagnostics are presented to evaluate the selected daily-based metrics. To reduce the number of figures in the core of the paper, some of them are presented in Supplementary Information (3 metrics in the core of the paper,

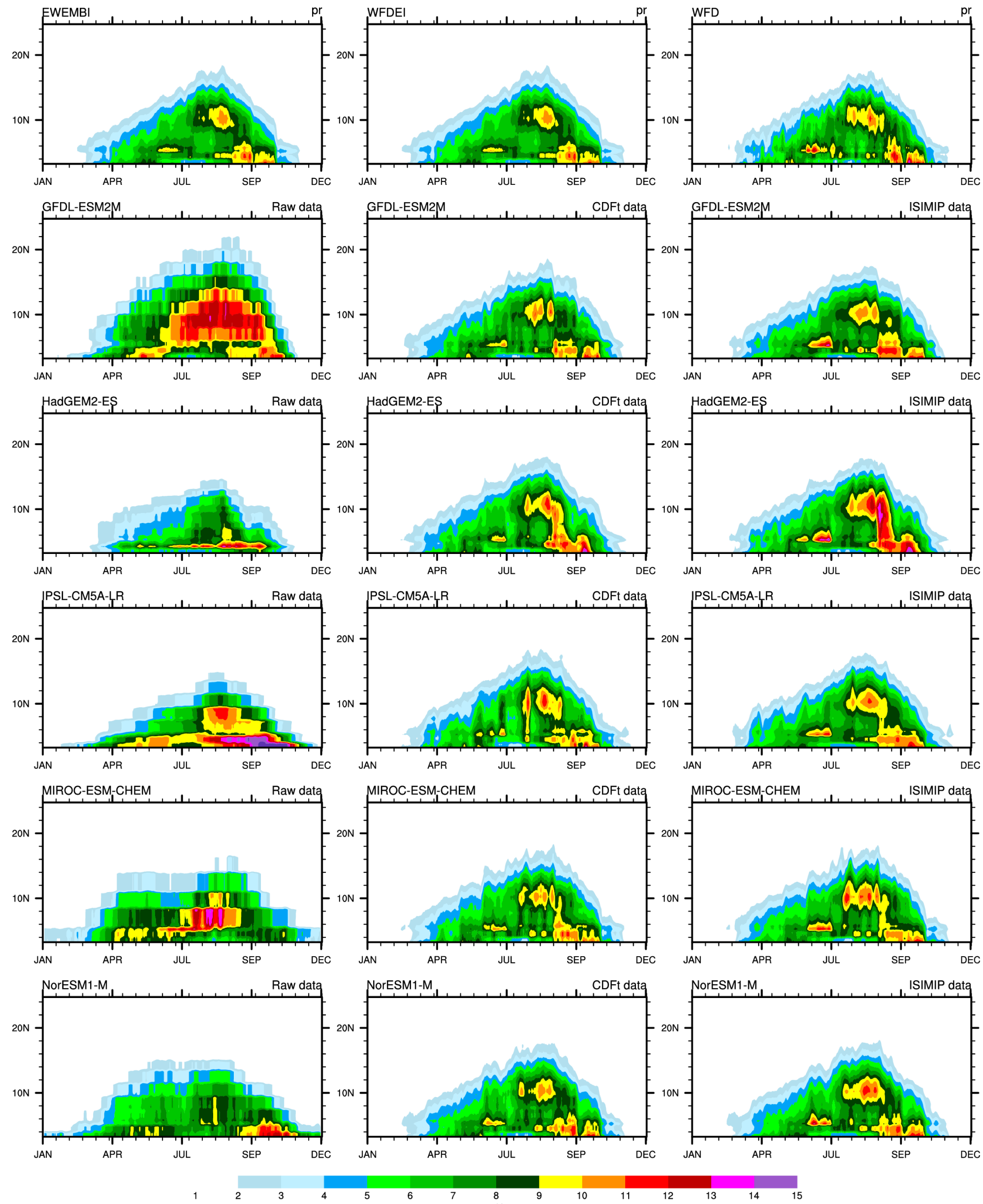

Figure 9. Same as Figure 8 but for precipitation rate in $\mathrm{mm\,day^{-1}}$

3 others in Supplementary Information). A more complete metrics report is available at http://www.amma2050.org/content/climate-metrics.

Fig.11 and Fig.12 shows the results for the tas 95$^{\text{th}}$ percentile of daily values of near-surface air temperature. WFD, WFDEI and EWEMBI provide similar values in summer (Fig.11 ; see also Table 2) with the highest values over Sahara in

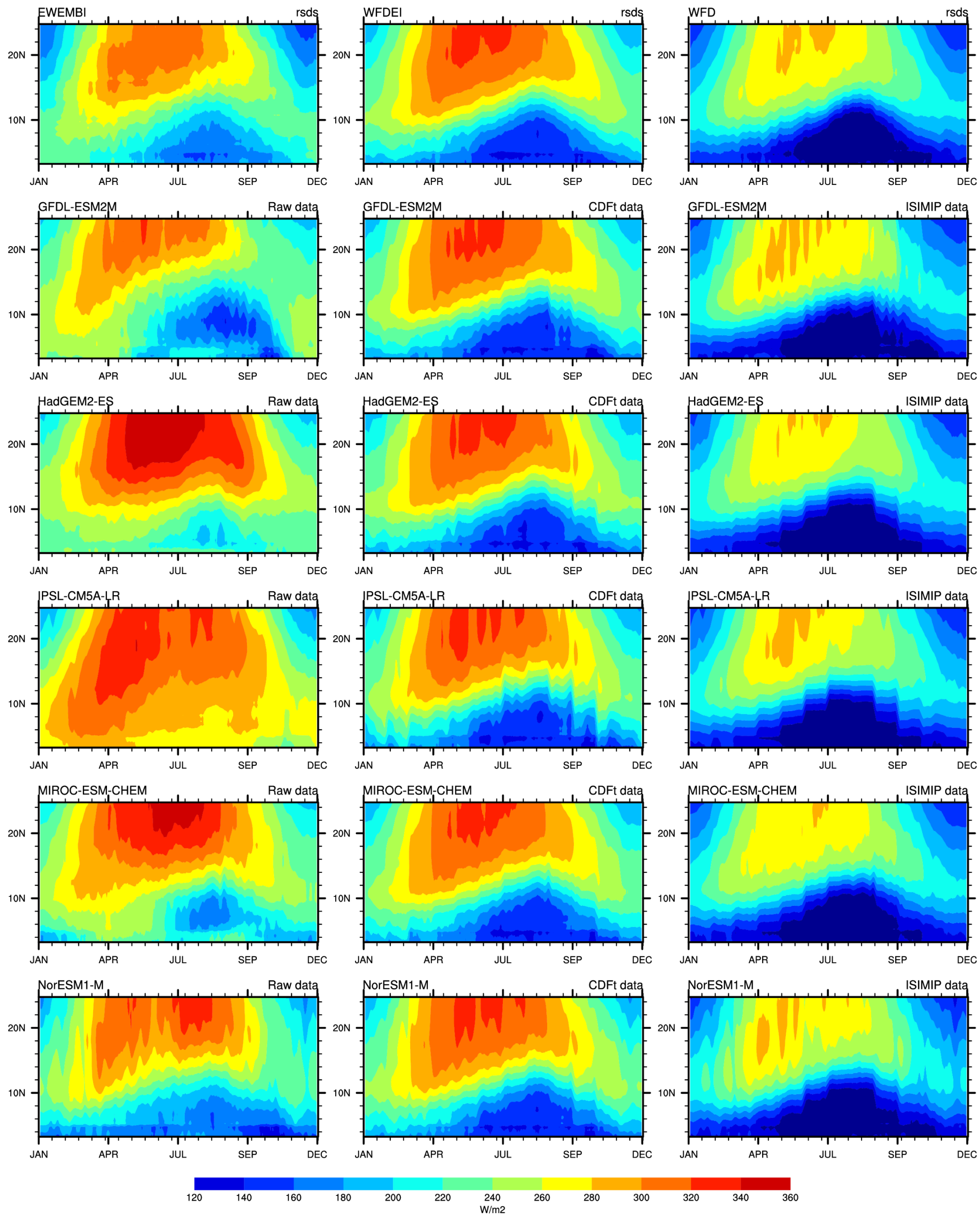

Figure 10. Same as Figure 8 but for solar radiation in $\mathrm{W\,m^{-2}}$

spring (up to 40°C, not shown), moving northward in summer, and with weaker values in fall (up to 32°C; not shown). WFD values appear a bit higher than the two other reference data sets. More to the south, in the Guinea area, the 95% percentile is between 30°C and 34°C. CDF-t bias-corrected data are also presented for the five GCMs used in ISIMIP in terms of differences relative to WFDEI. Some biases still remain but mostly lower than 1°C in absolute value. They are generally negative over the

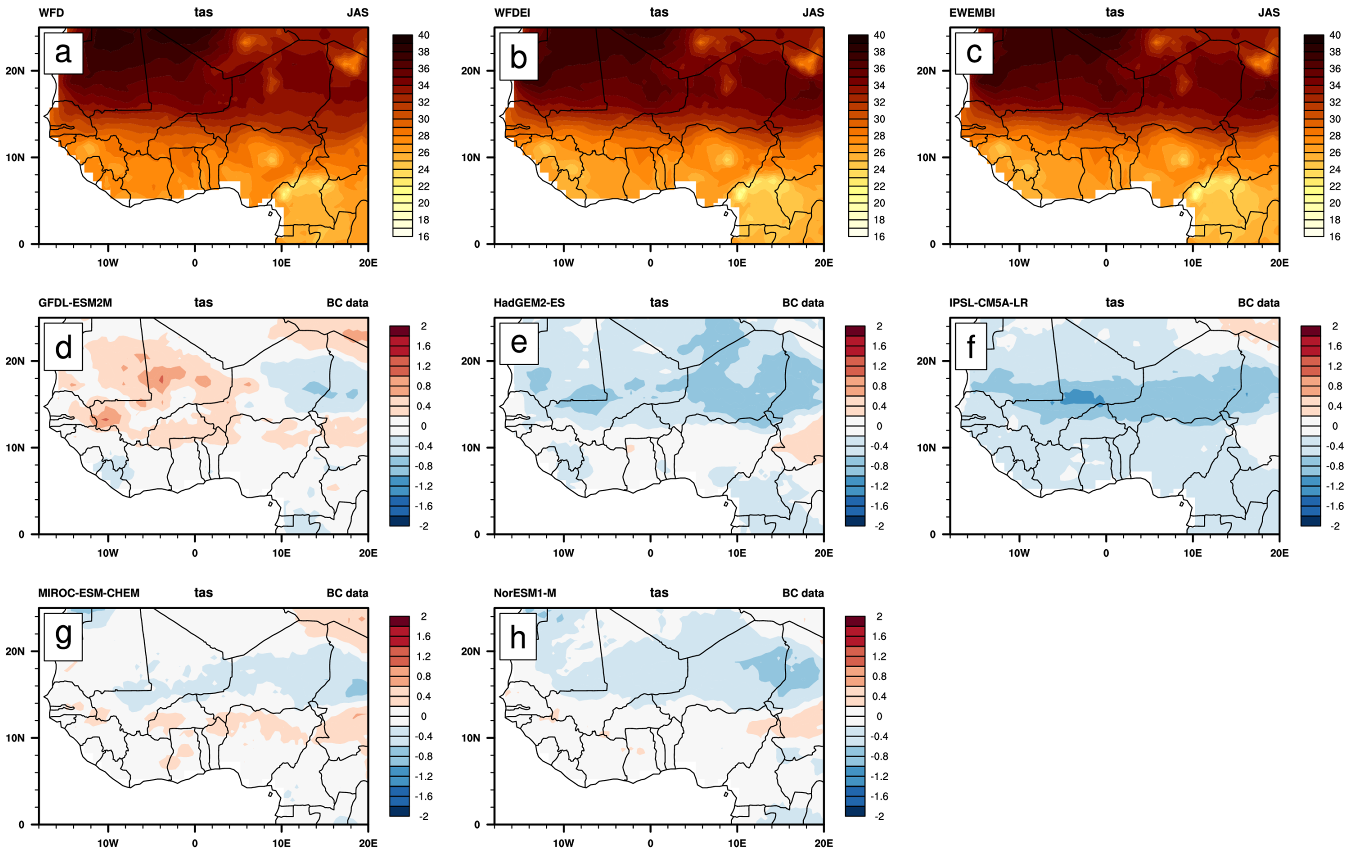

Figure 11. The 95th percentile of daily values for temperature from various observations dataset in JAS: WFD (a), WFDEI (b), EWEMBI (c) and difference relative to WFDEI data from 5 individual CDF-t bias-corrected models (d-h) over period 1979-2001

Sahara except for GFDL-ESM2M. The Taylor diagrams depict again the good performance of CDF-t bias-correction method here for extreme values. The highly scattered raw GCM data, especially over the Guinea area, move into a concentrated zone very near the WFDEI reference (Fig.12). ISIMIP bias-corrected data are also well concentrated near the WDF reference data but at some distance from WFDEI reference point. Here again, EWEMBI is superimposed to REF (see also Table 2), and bias-corrected GCMs are closer to REF for Sahel than for Guinea area.

Fig.13 and Fig.14 provide similar analysis for the 95th percentile of daily pr. WFD, WFDEI and EWEMBI provide fields consistent with the ITCZ location including high values over the mountain areas (Fig.13). WFDEI and EWEMBI have very similar fields while the range of values for WDF is very different, with values higher than 30 $\mathrm{mm\,day^{-1}}$ in the ITCZ in summer in contrast with values lower than 20 $\mathrm{mm\,day^{-1}}$ for the two other reference data sets (see also Table 2). Similar range of differences is present over the Guinea area in spring and to a lesser extent in fall (not shown). Such differences are also large over the mountain areas (Fouta Djalon, Cameroon). CDF-t bias-corrected GCMs data have remaining weak biases relative to WFDEI, lower than 2 $\mathrm{mm\,day^{-1}}$, except for IPSL-CM5A-LR where differences up to + 5 $\mathrm{mm\,day^{-1}}$ are located

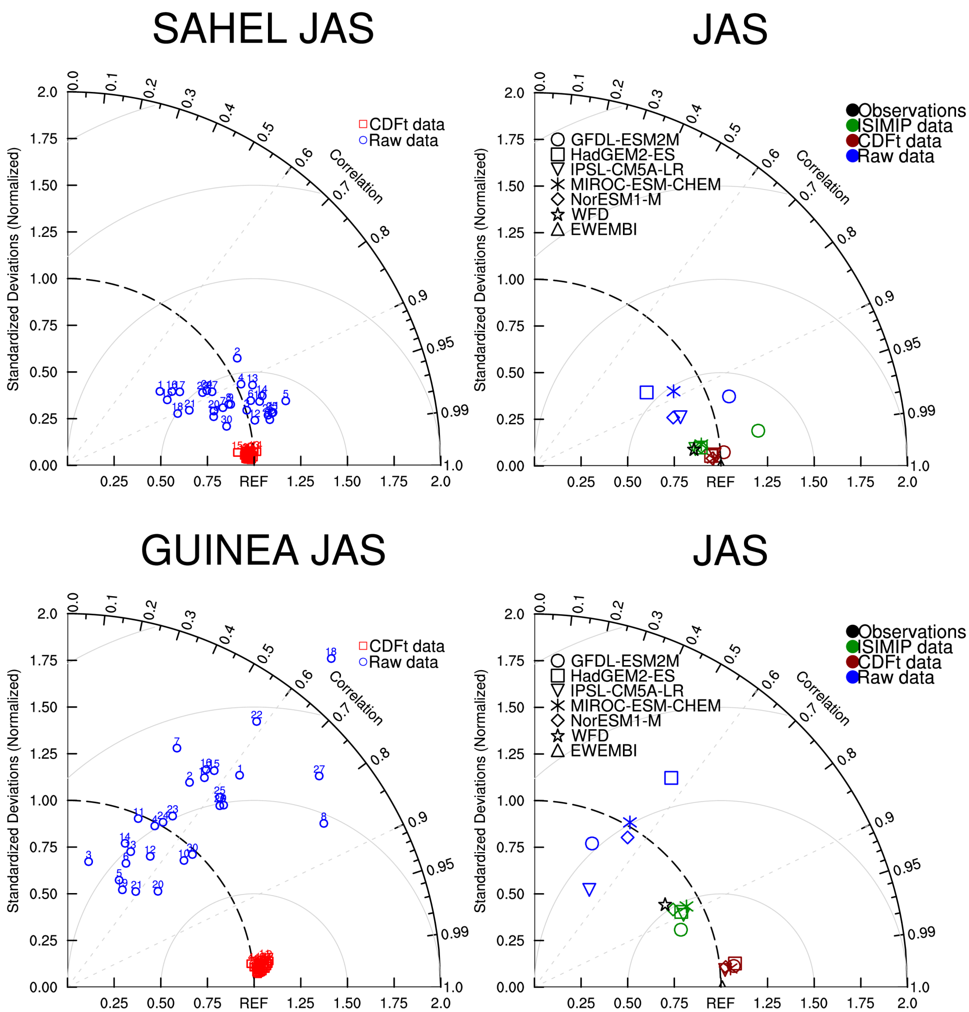

Figure 12. Same as Figure 3 but for the 95th percentile of near-surface temperature

north of 10°N. Compared to the 95th percentile of daily tas, Taylor diagrams (Fig.14) show again the good performance of the CDF-t bias-correction method for the 29 GCMs, but with a bit higher distance to REF both for Sahel and Guinea area. ISIMIP bias-corrected GCMs data are more scattered than CDF-t corrected GCMs in relative to their respective reference data set, WFD and WFDEI, and WFD is located far from WFDEI "REF" in terms of normalized standard deviation and centred RMSE (see also Tab.2).

Finally Fig.15 and Fig.16 provide similar analysis for the number of days with pr > 10 $\mathrm{mm\,day^{-1}}$. WFD, WFDEI and EWEMBI provide values consistent with the ITCZ location including high values over the mountain areas (Fig.15). In contrast to the previous metric, WFD has a more similar range of values relative to WFDEI and EWEMBI, with some over-estimation, especially over Nigeria, Cameroon and central Africa. The spatial variance is higher than for the two previous metrics with a higher contrast between mountain and plain areas. Remaining biases in the CDF-t corrected data are localised over mountain

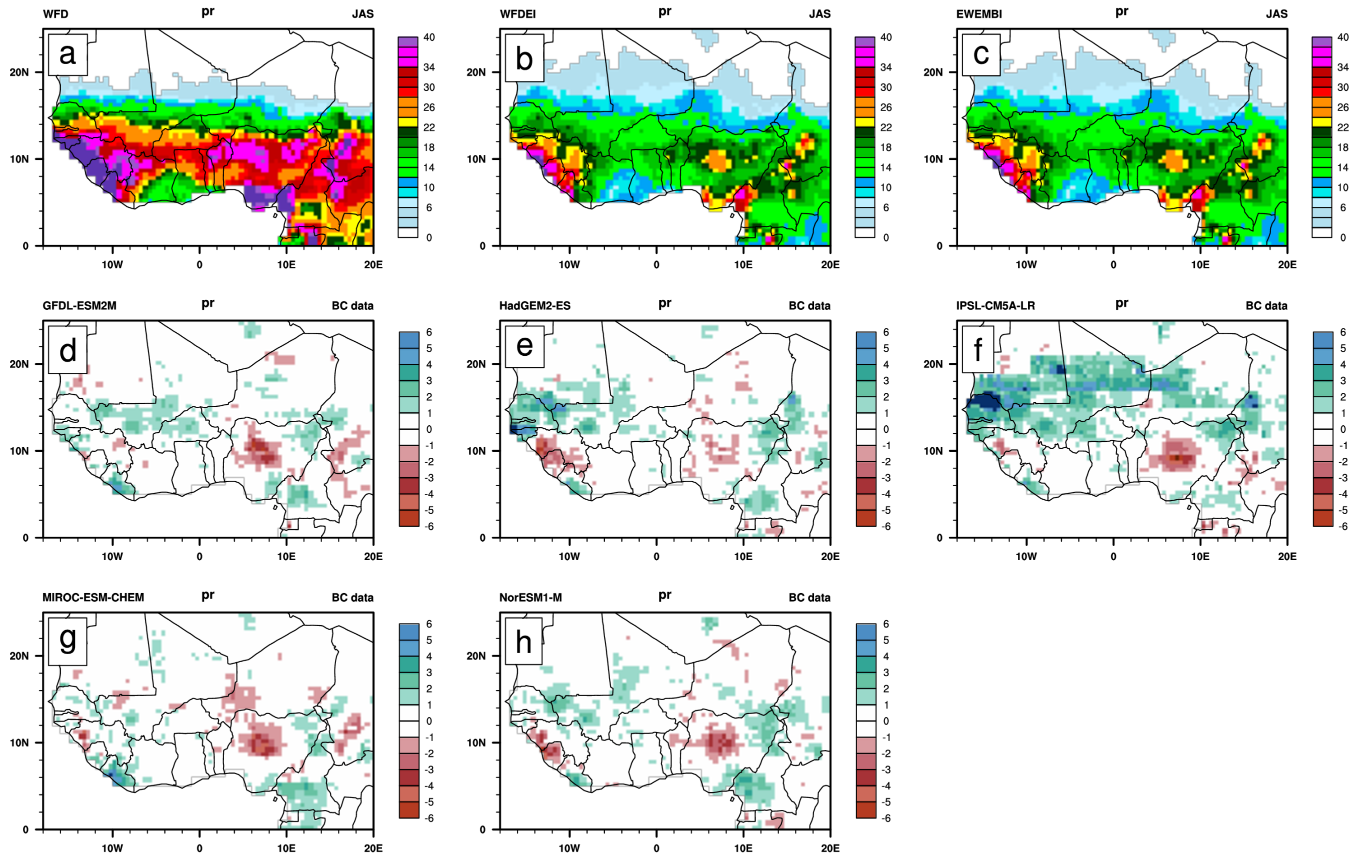

Figure 13. The 95$^{\text{th}}$ percentile of daily precipitation rate ($\mathrm{mm\,day^{-1}}$) from various observations dataset in JAS: WFD (a), WFDEI (b), EWEMBI (c) and difference relative to WFDEI data from 5 individual CDF-t bias-corrected models (d-h) over period 1979-2001

areas with mostly negative biases, but also over plains with mostly positive biases in the ITCZ area and especially extended for IPSL-CM5A-LR. Taylor diagrams (Fig.16) show once more a good performance of the CDF-t correction method to remove biases and reduce inter-GCMs dispersion. ISIMIP bias-corrected GCMs have a higher dispersion than CDF-t corrected GCMs relative to their respective reference data set.

4.4 Crop yields simulations and sensitivity to bias-corrected variables

The sensitivity of simulated crop yields over West Africa to raw and bias-corrected forcing data is now evaluated. A crop model forced by atmospheric variables integrates biases and variability of these forcing data in a non-linear way. This integration may reduce or amplify the variability induced from these forcing data.

This has been tested by using the crop model SARRA-O (System of Agroclimatological Regional Risk Analysis; version O). The model simulates yield attainable under water-limited conditions by simulating the soil water balance, potential and actual evapotranspiration, phenology, potential and water-limited carbon assimilation, and biomass partitioning (see Kouressy

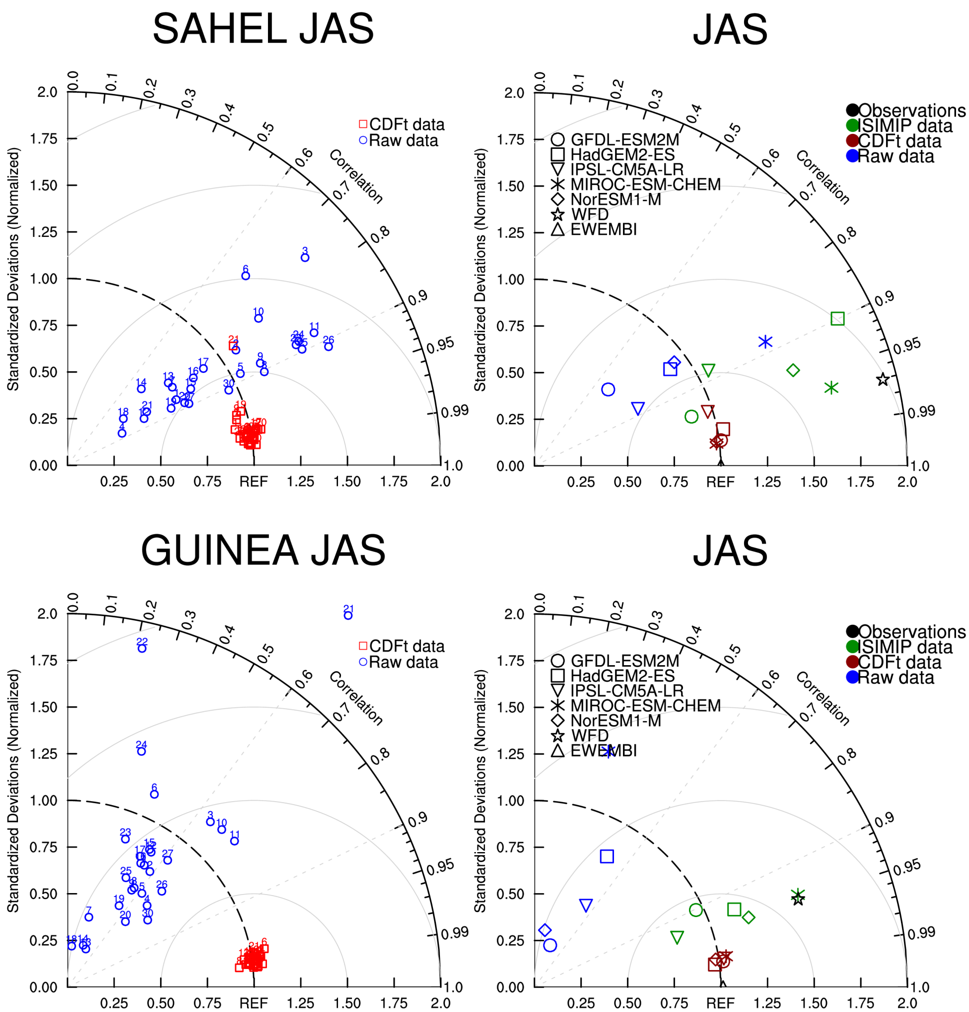

Figure 14. Same as Figure 3 but for the 95[th] percentile of daily precipitation rate ($\mathrm{mm\,day^{-1}}$)

et al., 2008, for a detailed review of model concepts). The simulation of these processes makes SARRA-O particularly suited for the analysis of climate impacts on cereal growth and yield in dry tropical environments (see for instance Sultan et al., 2013). Several sensitivity simulations have been carried out. First SARRA-O has been forced for each year from 1979 to 2001 by WFD, WFDEI and EWEMBI data. Second IPSL-CM5A-LR model has been used to force SARRA-O over the same years, with raw, CDF-t bias-corrected and ISIMIP bias-corrected data. The simulations have been compared to the "GDHY" data set (1981-2001) of 1.125°gridded yields estimation. "GDHY" are a hybrid of FAO country yield data, satellite-derived crop-specific vegetation index and global crop datasets on crop calendar, harvested area and production shares achieved by different growing season. Subnational yield statistics have been used to validate the grid-cell yield estimates (Iizumi et al., 2014). Note that SARRA-O provides potential yields that can be different from observed yields, so this comparison with the GDHY data set must be considered as indicative only. Finally, sensitivity to individual variables has been conducted by comparing the

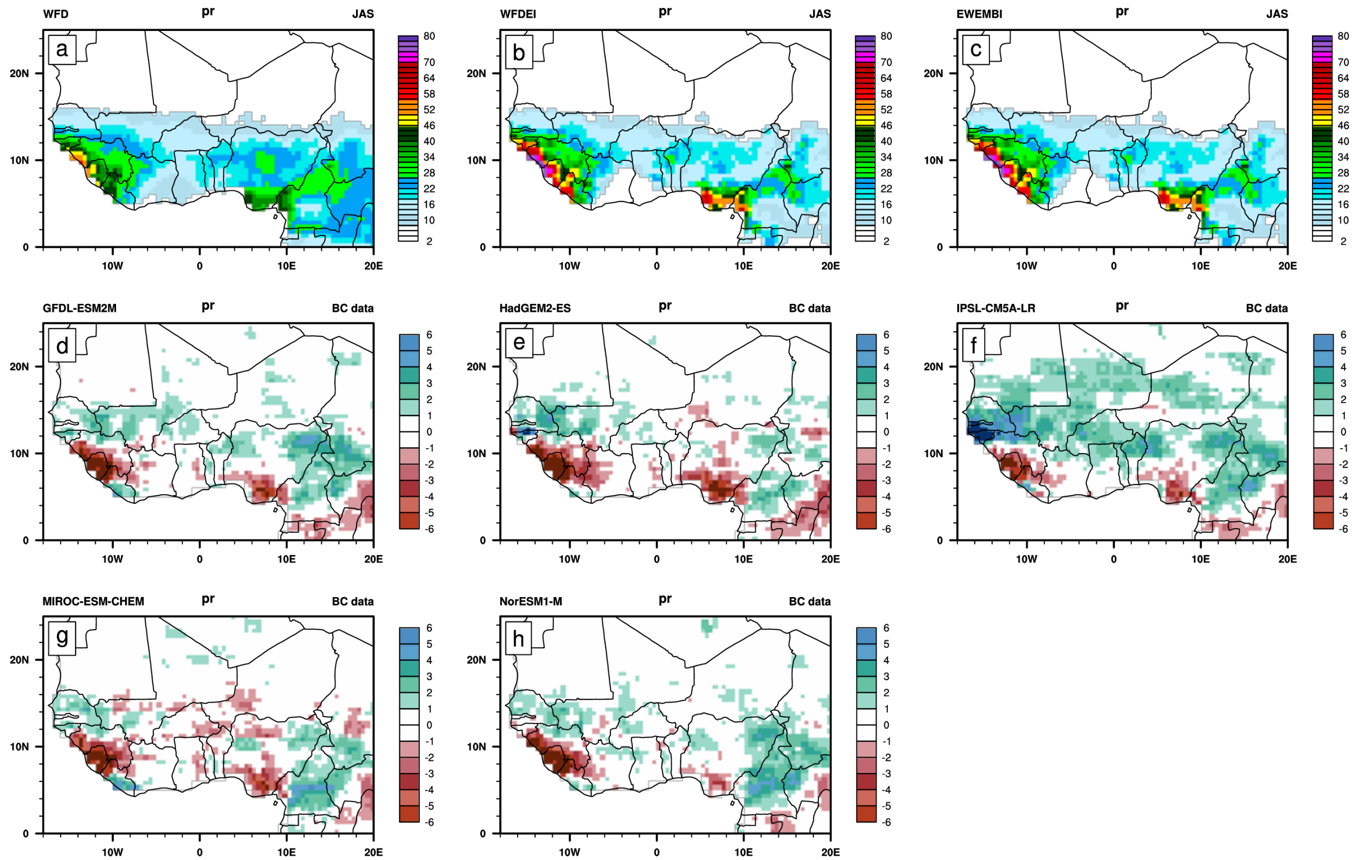

Figure 15. Seasonal mean of number of day with precipitation greater or equal to 10 $\mathrm{mm\,day^{-1}}$ from various observations dataset in JAS: WFD (a), WFDEI (b), EWEMBI (c) and difference relative to WFDEI data from 5 individual CDF-t bias-corrected models (d-h) over period 1979-2001

SARRA-O simulation forced with WFDEI data with simulations where one WFDEI variable is replaced by the corresponding raw IPSL-CM5A-LR data.

Fig.17 compares the simulated crop yields over the Sahel and Guinea areas when SARRA-O is forced either by WFD, WFDEI, EWEMBI, and by raw, CDF-t and ISIMIP bias-corrected IPSL-CM5A-LR model. GDHY data are also shown as evaluation. Over the Guinea area, the differentiation of ensembles of simulations is quite clear. Raw IPSL-CM5A-LR simulation has the highest yields (2200 $\mathrm{kg\,ha^{-1}}$) while WFD and associated ISIMIP bias-corrected simulations have the lowest yields (240 and 180 $\mathrm{kg\,ha^{-1}}$ respectively). The four remaining simulations, based on WFDEI and associated CDF-t bias-corrected data, EWEMBI and GDHY data, have intermediate yields, between 700 and 1000 $\mathrm{kg\,ha^{-1}}$. So it is shown first that SARRA-O maize yields are quite sensitive to the different forcing data sets, second that WFD leads to simulated yields far from the GDHY data while WFDEI and EWEMBI leads to quite better yields, and finally that raw GCM and GCM corrected with WFD are also quite far from the validation data while GCM corrected with WFDEI has a rather good performance. The

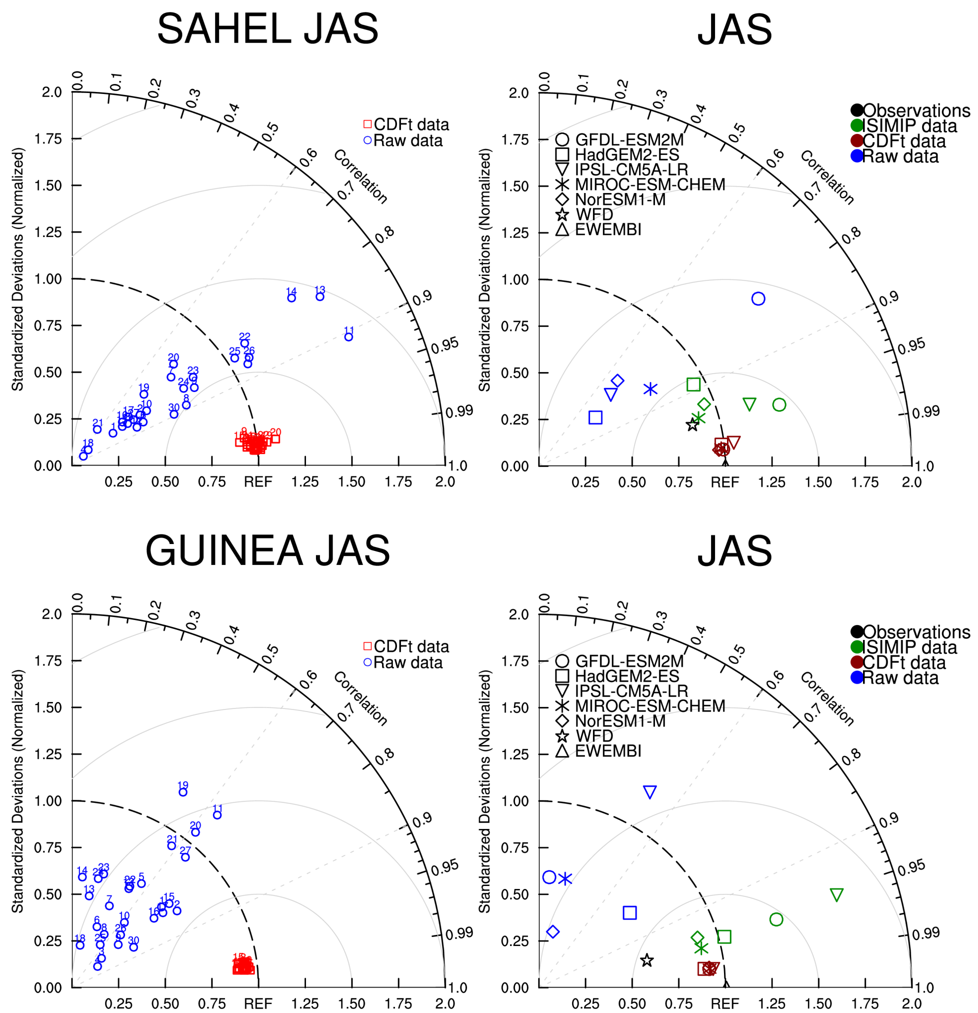

Figure 16. Same as Figure 3 but for number of day where precipitation is greater or equal to 10 $\mathrm{mm\,day^{-1}}$

simulation forced by EWEMBI has a higher mean value than WFDEI (760 and 1030 $\mathrm{kg\,ha^{-1}}$ respectively), and GDHY has yields ranging between WFDEI and EWEMBI (980 $\mathrm{kg\,ha^{-1}}$), close to EWEMBI. Over the Sahel area, the curves are closer but some similar conclusions can be drawn. WFD and associated ISIMIP bias-corrected simulations provide the lowest yields (400 and 370 $\mathrm{kg\,ha^{-1}}$ respectively). WFDEI, EWEMBI and CDF-t bias-corrected simulations are very close (660, 650 and 710 $\mathrm{kg\,ha^{-1}}$ respectively). Finally in contrast to the Guinea area, GDHY data has the highest yields (980 $\mathrm{kg\,ha^{-1}}$), far from other simulations. The raw simulation (590 $\mathrm{kg\,ha^{-1}}$) is close to WFDEI, EWEMBI and CDF-t bias-corrected simulations. This last point is quite surprising since raw IPSL-CM5A-LR data have large biases.

Fig.18 shows the maps of mean simulated yields for raw IPSL-CM5A-LR, WFDEI and CDF-t bias-corrected, EWEMBI simulations, GDHY data, and the difference between EWEMBI and WFDEI simulations. For raw simulations, yields are highly underestimated over the central Sahel but highly overestimated over the western Sahel and especially near the Fouta-

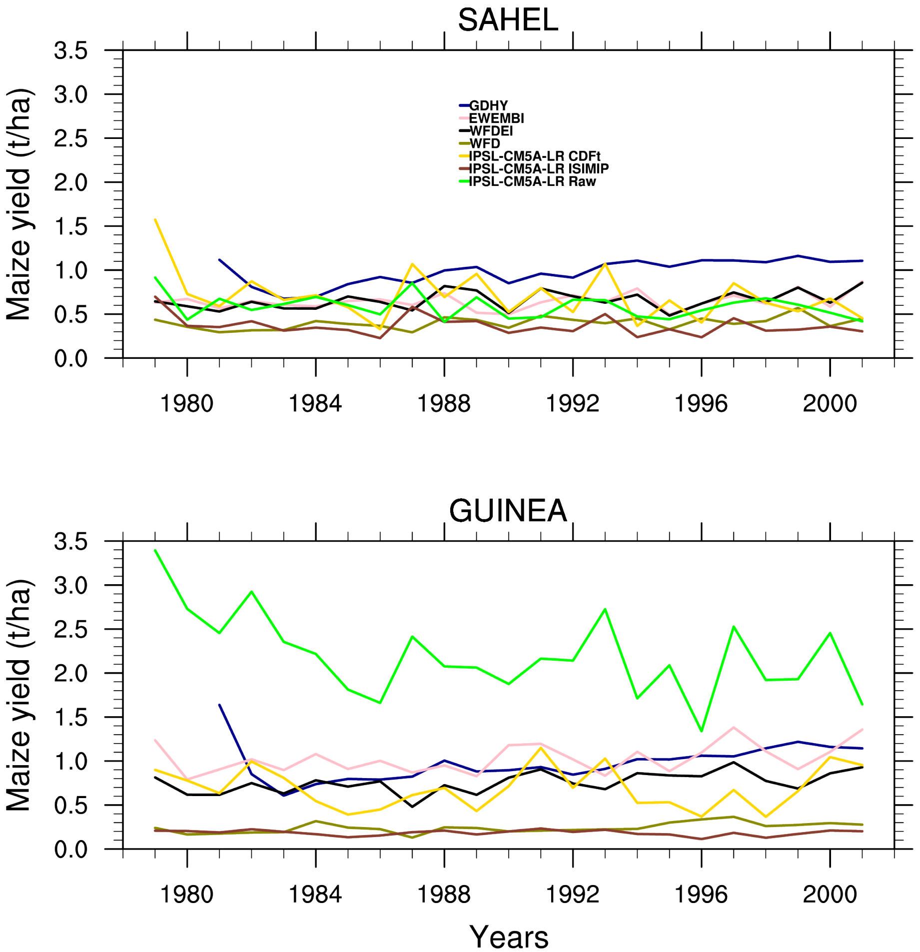

Figure 17. Time series of crop maize yield over Sahel box (18°W-10°E ; 10°N-20°N) and Guinea box (18°W-10°E ; 3°N-10°N) using IPSL-raw, IPSL-CDFt, IPSL-ISIMIP, and WFD, WFDEI, EWEMBI as forcing data over 1979-2001.

Jalon. The boundary between the Sahel and Guinea boxes being at 10°N, the spatial average over the Sahel combine positive and negative biases in respect to WFDEI. This explains the point raised at the end of the previous paragraph. The other maps show that yields obtained from EWEMBI are closer to GDHY data than yields from WFDEI, mostly due to better realistic values over the Guinea area (see also Table 3). Yields from EWEMBI are higher than yields from WFDEI mostly south of 10°N. Underestimation of yields simulated from WFDEI over Fouta-Jalon and over southern Cameroon and south-eastern Nigeria can be clearly associated with underestimation of WFDEI rsds compared to EWEMBI rsds (see Fig.1). Comparisons on WFDEI and EWEMBI interannual time series of yields and associated tas, pr and rsds on individual grid points in these areas confirm that these yields differences are linked exclusively to rsds differences. Finally maps of simulated yields from WFD and ISIMIP bias-correction confirm the weak values over the whole West Africa due to an under-estimation of rsds south of 10°N (not shown).

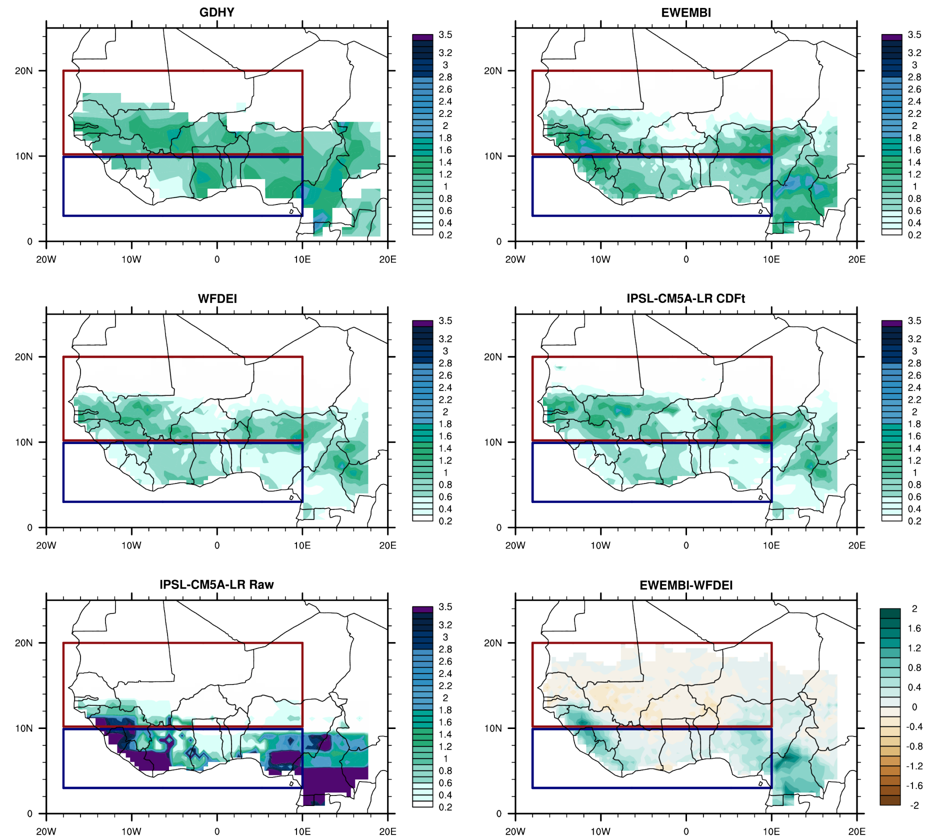

Figure 18. Temporal mean of maize yield (in t/ha) for IPSL-raw, IPSL-CDF-t, WFDEI, EWEMBI, GDHY over 1979-2001 and the difference between EWEMBI and WFDEI simulations. The boxes indicates Sahel (18°W-10°E ; 10°N-20°N) and Guinea (18°W-10°E ; 3°N-10°N) regions.

To go further, a sensitivity analysis to individual variables has been conducted by comparing the SARRA-O simulation forced with WFDEI data with simulations where one of these WFDEI variables is replaced by the corresponding raw IPSL-CM5A-LR data. These variables are pr, rsds, tasmin and tasmax, and also rsds from ISIMIP bias-corrected IPSL-CM5A-LR (using WFD as reference). Table 3 shows the mean yields for the Sahel and Guinea areas and the resulting biases relative to WFDEI simulations. Biases are very weak with tasmin-tasmax simulations (WFDEItminmax), a bit higher for pr simulations (WFDEIpr), then for rsds, (WFDEIrsds) and drastically large for rsds from ISIMIP bias-corrected simulations (WFDEIWFDrsds). So rsds appears as a very critical variable for maize yields simulated with SARRA-O, confirming a previous study based on an older version SARRA-H of crop model (Oettli et al., 2011).

SARRA-O has also been run over the period 1950-2099 using the RCP8.5 projection, forced by ISPL-CM5A-LR in terms of raw, CDF-t bias-corrected and ISIMIP bias-corrected data. Fig.19 shows on one hand the resulting time series of maize yields over the Sahel and Guinea boxes, and on another hand the maps of yields from CDF-t bias-corrected data over 1979-2001, 2077-2099, and the resulting difference between these two periods. Time series of standardized yields anomalies

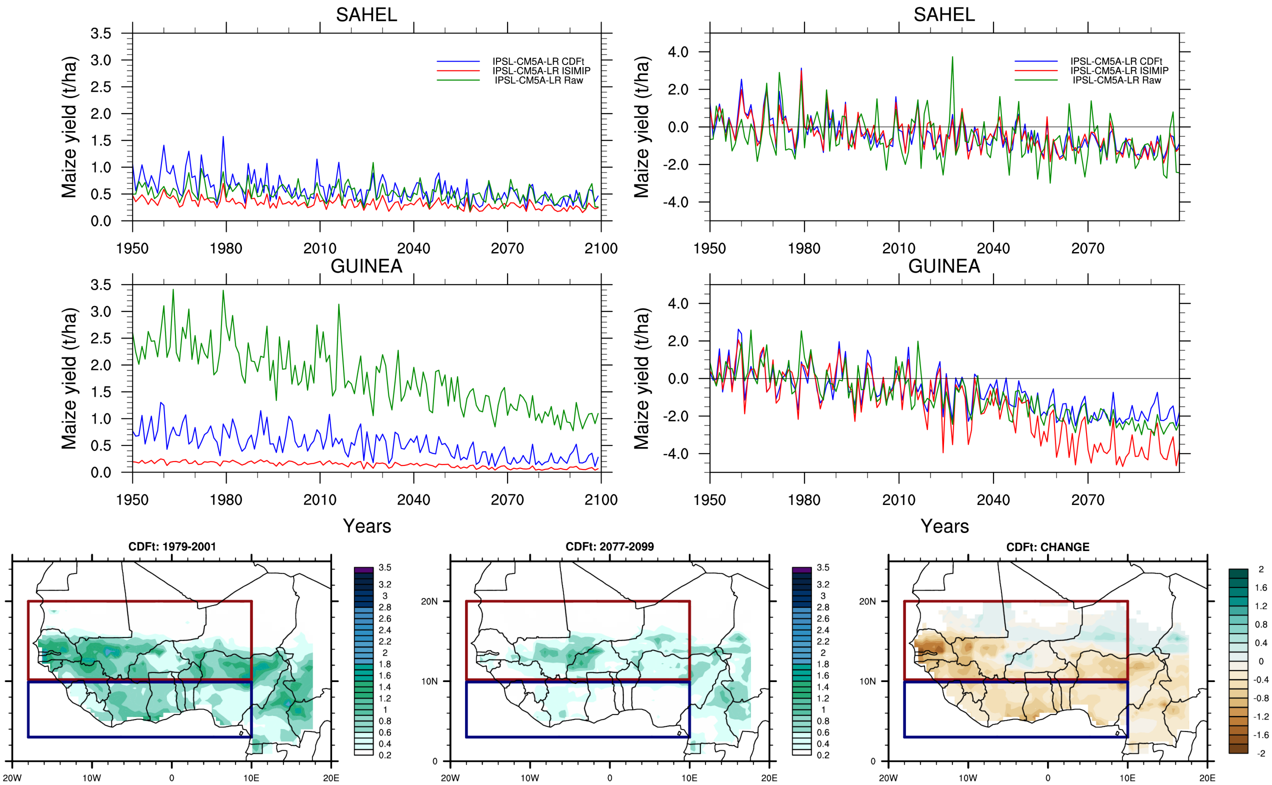

Figure 19. Time series of RCP8.5 projections of maize yields over Sahel box (18°W-10°E ; 10°N-20°N) and Guinea box (18°W-10°E ; 3°N-10°N) (left column) and yields standardized anomalies to their respective mean over 1979-2001 (right column), using IPSL-CM5A-LR raw data (green line), BC data with CDF-t (blue line) and ISIMIP BC data (red line) as forcing data. Maps show mean maize yields from CDF-t bias-corrected data over 1979-2001, 2077-2099, and their difference.

to their respective mean over 1979-2001 are also displayed. In agreement with the previous analysis, ISIMIP bias-corrected forcing data (with WFD as reference data) lead to the lowest yields both over the Sahel and Guinea areas on the present time but also over the whole 21st century. Over Guinea area, the very high simulated yields coming from raw data are drastically reduced with CDF-t bias-corrected forcing data (with WFDEI as reference data) while over the Sahel area these yields are rather similar. After CDF-t bias-correction, yields are quite similar over the two areas. Interannual variability of simulated yields is proportional to the mean with a very weak variability for ISIMIP yield and higher variability for CDF-t and raw simulations. More precisely, standardized yield anomalies (right panels) have a similar range over the Sahel, around one standard deviation after 2060, and a range around two standard deviations after 2070 over the Guinea area except ISIMIP yields that reach four standard deviations. All projections show a clear decrease of maize yields by a factor of 2 over all of West Africa along the 21st century. The map of the difference between 2077-2099 and 1979-2001 shows that the yield decrease is located mostly south of 13°N except between Mali and Niger, and that a slight increase is present north of 13°N.

Table 3. Sensitivity experiments means and biases (in $\mathrm{kg\,ha^{-1}}$) in respect to WFDEI simulations for the Sahel and Guinea areas. Sensitivity simulations to individual variables have been conducted by forcing the SARRA-O model with WFDEI data, and by replacing one of the WFDEI variables by the corresponding raw IPSL-CM5A-LR data. These variables are pr, rsds, tasmin and tasmax, and also rsds from ISIMIP bias-corrected IPSL-CM5A-LR (using WFD as reference).

	SAHEL		**GUINEA**	
	Mean	**Bias**	**Mean**	**Bias**
WFDEI	658	0	757	0
WFD	398	-260	241	-516
EWEMBI	646	-12	1029	272
GDHY	979	321	978	221
IPSL-CM5A-LR Raw	586	-72	2201	1444
IPSL-CM5A-LR CDFt	706	48	693	-64
IPSL-CM5A-LR ISIMIP	367	-291	184	-573
WFDEIpr	668	10	716	-41
WFDEIrsds	717	59	786	29
WFDEItminmax	658	0	767	10
WFDEIWFDrsds	317	-341	195	-562

5 Conclusions

The objectives of this paper are (i) to introduce a new bias-corrected dataset whose the CDF-t correction method has been applied on CMIP5 GCMs daily data for the first time over Africa, (ii) to quantify the effect of using different reference datasets on the corrected data, (iii) and to illustrate this effect on crop simulations over West Africa. This bias-correction has been applied over the period 1950-2099 combining historical runs and RCP scenarios with 29/27/20 GCMs for RCP8.5/4.5/2.6 respectively. It have been applied on six variables critical for agricultural impacts, daily accumulated precipitation, daily mean, minimum and maximum near-surface air temperature, daily mean surface downwelling shortwave and daily mean wind speed.

The use of different bias-correction methods based also on different reference data sets contributes to the total uncertainty in climate projections and can contribute in some contexts more than the use of different GCMs or RCMs (Iizumi et al., 2017). So using multiple bias-correction technics and reference data sets is highly recommended. In this context, CDF-t bias-corrected GCM data have been compared to the 5 GCMs ISIMIP bias-corrected data, and the impact of the different reference data sets, WFD (used in ISIMIP bias-corrections), WFDEI (used in CDF-t bias-corrections) and the more recent EWEMBI (used in a second version of ISIMIP bias-corrections), has been examined in details. Crop simulations have been also carried out to test how the impact of bias-corrections in forcing data (temperature, precipitation, surface down-welling shortwave radiation) is integrated in terms of crop (maize) yields. Finally bias-corrections have also been presented in the context of RCP8.5 scenarios.

The whole observational period, 1979-2013, has been chosen to calibrate the bias-correction process. It has been shown that using various calibration sub-periods has a weak impact in particular on the time evolution over the 21st century.

The evaluation of CDF-t bias-correction applied to the 29 GCMs, both on mean seasonal data and on daily-based metrics, has shown that CDF-t is very effective in removing the biases in respect to the reference WFDEI data and in reducing the high inter-GCMs scattering. It has also shown some distance, depending on variables and metrics, with bias-corrected ISIMIP GCM data, mainly due to the differences between WFDEI and WFD reference data. WFDEI (and associated CDF-t bias-corrected GCMs) appears closer to EWEMBI than WFD (and associated ISIMIP bias-corrected GCMs). Metrics based on temperature are very close for the three reference data sets, and some differences exist in precipitation-based metrics. In contrast, significant differences have been highlighted in terms of surface down-welling shortwave radiation. This has consequences in terms of crop (maize) yields over West Africa. Sensitivity simulations performed with one GCM have shown that bias-corrections improve the yields simulated by the raw GCM. However ISIMIP bias-corrected GCM still underestimate them as CDF-t bias-corrected GCM do but with yield estimates closer to observed ones. EWEMBI provides the closest yields to observed estimates. This is mainly due to surface down-welling shortwave radiation whose values are under-estimated in WFDEI south of 10°N. Finally, in agreement with maize yield sensitivity simulations, projections of future yields over West Africa have quite different levels depending on bias-correction method. However they show all a similar relative decreasing trend over the 21st century.

The main perspective of this work is to go on exploring the uncertainty linked to bias-correction methods and their associated reference data in RCP climate scenarios by producing a second version of this bias-corrected 29 GCMs ensemble over Africa using more recent reference data like EWEMBI, or others as those used in AgMIP based on other reanalyses (AgMERRA or AgCFSR, (Ruane et al., 2015)). The main divergence between all those reference data sets are probably expected from surface down-welling shortwave radiation. Bias-correction for other variables useful for user-based metrics as specific humidity is also scheduled. Comparison between CDF-t and ISIMIP bias-corrections methods based on the same reference data set is also on-going.

The CFD-t bias-correction has been applied independently for each of the six variables. However this may be a problem since existing spatial coherency and dependence among variables maybe destroyed by the application of univariate calibrations. Recently, to address this issue, improved calibrations have been developed in terms of multivariate correction, spatial and/or temporal dependences (see for instance Vrac and Friederichs, 2015, for a synthesis). Implementation of more sophisticated methods using multivariate correction is also on-going.

This work constitutes a first step in producing bias-corrected data sets over Africa within AMMA-2050. An atlas is in preparation that will provide extensive results over Africa to the FCFA stakeholders and end-users communities. These communities will be accompanied by FCFA climate scientists in order to be aware of the way to use these data and their limitations.

Acknowledgements. The research leading to these results has received partial funding from the NERC/DFID Future Climate For Africa programme under the AMMA-2050 project, grant number NE/M019934/1. The lead author has been also supported by IRD. M. V. has been partly funded by the ANR StaRMIP project. We acknowledge the World Climate Research Programme's Working Group on Coupled Modelling, which is responsible for CMIP, and we thank the climate modelling groups (listed in Table1 of this paper) for producing and making available their model output. For CMIP the U.S. Department of Energy's Program for Climate Model Diagnosis and Intercomparison provides coordinating support and led development of software infrastructure in partnership with the Global Organization for Earth System Science Portals. The authors thank also EU Watch project and its members for data availability and ISIMIP data (doi:10.5880/PIK.2016.001 for ISIMIP Fast Track and http://doi.org/10.5880/pik.2016.004 for EWEMBI dataset). The CDF-t bias-corrected CMIP5 data over Africa is currently under embargo. Upon the expiration of the embargo the data will be made available by the AMMA-2050 project.

References

Dee, D. P., Uppala, S. M., Simmons, A. J., Berrisford, P., Poli, P., Kobayashi, S., Andrae, U., Balmaseda, M. A., Balsamo, G., Bauer, P., Bechtold, P., Beljaars, A. C. M., van de Berg, L., Bidlot, J., Bormann, N., Delsol, C., Dragani, R., Fuentes, M., Geer, A. J., Haimberger, L., Healy, S. B., Hersbach, H., Hólm, E. V., Isaksen, L., Kållberg, P., Köhler, M., Matricardi, M., McNally, A. P., Monge-Sanz, B. M., Morcrette, J.-J., Park, B.-K., Peubey, C., de Rosnay, P., Tavolato, C., Thépaut, J.-N., and Vitart, F.: The ERA-Interim reanalysis: configuration and performance of the data assimilation system, Quarterly Journal of the Royal Meteorological Society, 137, 553–597, https://doi.org/10.1002/qj.828, http://doi.wiley.com/10.1002/qj.828, 2011.

Déqué, M.: Frequency of precipitation and temperature extremes over France in an anthropogenic scenario: model results and statistical correction according to observed values, Global and Planetary Change, 57, 16–26, 2007.

Dutra, E.: Report on the current state-of-the-art Water Resources Reanalysis, Tech. rep., Tech. Rep. D, 2015.

Frieler, K., Lange, S., Piontek, F., Reyer, C. P., Schewe, J., Warszawski, L., Zhao, F., Chini, L., Denvil, S., Emanuel, K., et al.: Assessing the impacts of 1.5 C global warming–simulation protocol of the Inter-Sectoral Impact Model Intercomparison Project (ISIMIP2b), Geoscientific Model Development, 10, 4321, 2017.

Hagemann, S., Chen, C., Haerter, J. O., Heinke, J., Gerten, D., and Piani, C.: Impact of a statistical bias correction on the projected hydrological changes obtained from three GCMs and two hydrology models, Journal of Hydrometeorology, 12, 556–578, 2011.

Hempel, S., Frieler, K., Warszawski, L., Schewe, J., and Piontek, F.: A trend-preserving bias correction–the ISI-MIP approach, Earth System Dynamics, 4, 219–236, 2013.

Iizumi, T., Yokozawa, M., Sakurai, G., Travasso, M. I., Romanenkov, V., Oettli, P., Newby, T., Ishigooka, Y., and Furuya, J.: Historical changes in global yields: major cereal and legume crops from 1982 to 2006, Global ecology and biogeography, 23, 346–357, 2014.

Iizumi, T., Takikawa, H., Hirabayashi, Y., Hanasaki, N., and Nishimori, M.: Contributions of different bias-correction methods and reference meteorological forcing data sets to uncertainty in projected temperature and precipitation extremes, Journal of Geophysical Research: Atmospheres, 2017.

Kallache, M., Vrac, M., Naveau, P., and Michelangeli, P.-A.: Nonstationary probabilistic downscaling of extreme precipitation, Journal of Geophysical Research: Atmospheres, 116, 2011.

Kouressy, M., Dingkuhn, M., Vaksmann, M., and Heinemann, A. B.: Adaptation to diverse semi-arid environments of sorghum genotypes having different plant type and sensitivity to photoperiod, Agricultural and Forest Meteorology, 148, 357–371, 2008.

Lange, S.: EartH2Observe, WFDEI and ERA-Interim data Merged and Bias-corrected for ISIMIP (EWEMBI), GFZ Data Serv, 2016.

Lange, S.: ISIMIP2 bias-correction fact sheet., http://www.isimip.org, 2017a.

Lange, S.: Bias correction of surface downwelling longwave and shortwave radiation for the EWEMBI dataset, Earth System Dynamics Discussions, 2017, 1–30, https://doi.org/10.5194/esd-2017-81, https://www.earth-syst-dynam-discuss.net/esd-2017-81/, 2017b.

Lavaysse, C., Flamant, C., Janicot, S., Parker, D. J., Lafore, J.-P., Sultan, B., and Pelon, J.: Seasonal evolution of the West African heat low: a climatological perspective, Climate Dynamics, 33, 313–330, https://doi.org/10.1007/s00382-009-0553-4, http://link.springer.com/10.1007/s00382-009-0553-4, 2009.

Lavaysse, C., Vrac, M., Drobinski, P., Lengaigne, M., and Vischel, T.: Statistical downscaling of the French Mediterranean climate: assessment for present and projection in an anthropogenic scenario, Natural Hazards and Earth System Science, 12, 651–670, 2012.

Meehl, G. A., Boer, G. J., Covey, C., Latif, M., and Stouffer, R. J.: The coupled model intercomparison project (CMIP), Bulletin of the American Meteorological Society, 81, 313–318, 2000.

Michelangeli, P.-A., Vrac, M., and Loukos, H.: Probabilistic downscaling approaches: Application to wind cumulative distribution functions, Geophysical Research Letters, 36, 2009.

Moss, R. H., Edmonds, J. A., Hibbard, K. A., Manning, M. R., Rose, S. K., Van Vuuren, D. P., Carter, T. R., Emori, S., Kainuma, M., Kram, T., et al.: The next generation of scenarios for climate change research and assessment, Nature, 463, 747–756, 2010.

Oettli, P., Sultan, B., Baron, C., and Vrac, M.: Are regional climate models relevant for crop yield prediction in West Africa?, Environmental Research Letters, 6, 014 008, 2011.

Roehrig, R., Bouniol, D., Guichard, F., Hourdin, F., and Redelsperger, J.-L.: The present and future of the West African monsoon: a process-oriented assessment of CMIP5 simulations along the AMMA transect, Journal of Climate, 26, 6471–6505, 2013.

Ruane, A. C., Goldberg, R., and Chryssanthacopoulos, J.: Climate forcing datasets for agricultural modeling: Merged products for gap-filling and historical climate series estimation, Agricultural and Forest Meteorology, 200, 233–248, 2015.

Stackhouse Jr, P. W., Gupta, S. K., Cox, S. J., Zhang, T., Mikovitz, J. C., and Hinkelman, L. M.: The NASA/GEWEX surface radiation budget release 3.0: 24.5-year dataset, GEWEX News, 21, 10–12, 2011.

Sultan, B. and Janicot, S.: The West African Monsoon Dynamics. Part II: The "Preonset" and "Onset" of the Summer Monsoon, Journal of Climate, 16, 3407–3427, https://doi.org/10.1175/1520-0442(2003)016<3407:TWAMDP>2.0.CO;2, http://journals.ametsoc.org/doi/abs/10.1175/1520-0442%282003%29016%3C3407%3ATWAMDP%3E2.0.CO%3B2, 2003.

Sultan, B., Roudier, P., Quirion, P., Alhassane, A., Muller, B., Dingkuhn, M., Ciais, P., Guimberteau, M., Traore, S., and Baron, C.: Assessing climate change impacts on sorghum and millet yields in the Sudanian and Sahelian savannas of West Africa, Environmental Research Letters, 8, 014 040, 2013.

Taylor, K. E.: Summarizing multiple aspects of model performance in a single diagram, Journal of Geophysical Research: Atmospheres, 106, 7183–7192, 2001.

Taylor, K. E., Stouffer, R. J., and Meehl, G. A.: An Overview of CMIP5 and the Experiment Design, Bulletin of the American Meteorological Society, 93, 485–498, https://doi.org/10.1175/BAMS-D-11-00094.1, http://journals.ametsoc.org/doi/abs/10.1175/BAMS-D-11-00094.1, 2012.

Vautard, R., Noël, T., Li, L., Vrac, M., Martin, E., Dandin, P., Cattiaux, J., and Joussaume, S.: Climate variability and trends in downscaled high-resolution simulations and projections over Metropolitan France, Climate dynamics, 41, 1419–1437, 2013.

Vigaud, N., Vrac, M., and Caballero, Y.: Probabilistic downscaling of GCM scenarios over southern India, International Journal of Climatology, 33, 1248–1263, 2013.

Vrac, M. and Friederichs, P.: Multivariate—intervariable, spatial, and temporal—bias correction, Journal of Climate, 28, 218–237, 2015.

Vrac, M., Drobinski, P., Merlo, A., Herrmann, M., Lavaysse, C., Li, L., and Somot, S.: Dynamical and statistical downscaling of the French Mediterranean climate: uncertainty assessment, Natural Hazards and Earth System Sciences, 12, 2769–2784, 2012.

Vrac, M., Noël, T., and Vautard, R.: Bias correction of precipitation through Singularity Stochastic Removal: Because occurrences matter, Journal of Geophysical Research: Atmospheres, 2016.

Weedon, G., Gomes, S., Viterbo, P., Shuttleworth, W. J., Blyth, E., Österle, H., Adam, J., Bellouin, N., Boucher, O., and Best, M.: Creation of the WATCH forcing data and its use to assess global and regional reference crop evaporation over land during the twentieth century, Journal of Hydrometeorology, 12, 823–848, 2011.

Weedon, G. P., Balsamo, G., Bellouin, N., Gomes, S., Best, M. J., and Viterbo, P.: The WFDEI meteorological forcing data set: WATCH Forcing Data methodology applied to ERA-Interim reanalysis data, Water Resources Research, 50, 7505–7514, 2014.